ANALYZING "HOT SPOTS" CREATED BY ELECTRON BEAM (EBEAM) TECHNOLOGY

An Undergraduate Research Scholars Thesis

by

ARACELY ANAHI PEREZ GOMEZ

Submitted to the Undergraduate Research Scholars program at
Texas A&M University
in partial fulfillment of the requirements for the designation as an

UNDERGRADUATE RESEARCH SCHOLAR

Approved by Research Advisor: Dr. Suresh D. Pillai

May 2019

Major: Molecular and Cell Biology

TABLE OF CONTENTS

ABSTRACT

Analyzing “Hot Spots” Created by Electron Beam (eBeam) Technology

Aracely Anahi Perez Gomez
Department of Biology
Texas A&M University

Research Advisor: Dr. Suresh D. Pillai
Department of Poultry Science/Food Science
Texas A&M University

Electron beam (eBeam) technology is commonly used to sterilize food and food ingredients to inactivate microbial pathogens. In eBeam processing, electrons are accelerated to the speed of light in a linear accelerator, before being showered over a product, resulting in microbial inactivation. It causes multiple single and double strand breaks in the DNA of microbial pathogens and other organisms that may be present. If the cell undergoes numerous double-strand DNA breaks, the bacterium is considered inactivated because it can no longer multiply. When exposed to electron beam (eBeam) irradiation it has been observed that bacterial genomE undergoes fragmentation. However, it is unclear whether there are “hot spots” in the genome for these DNA breakages. It is important to understand whether “hotspots” exist that help create these breakages when DNA encounters electrons. These studies can lead to a better understanding of the effects eBeam has on bacterial DNA. This will also help to determine how bacterial cells respond to eBeam irradiation. *E. coli* and *Salmonella* cells were exposed to a kill dose of eBeam irradiation to measure differences in physical damage. The experimental objective was to determine whether eBeam creates random DNA breakages or if there are “hot spots” where the double stranded DNA breaks occur.

ACKNOWLEDGEMENTS

I would like to thank my committee chair, Dr. Suresh D. Pillai, and my mentor, Sohini Bhatia, and my colleges for their guidance and support throughout the course of this research. I appreciate the time they have taken to mentor and assist me while also working on their own projects. I am grateful for the eBeam staff, Mickey Speakmon and Sara Parsons, for assisting me at the National Center for Electron Beam Research. I would also like to thank the Texas A&M Genomics and Bioinformatics Center for aiding when measuring all my samples. Finally, I would like to thank my family and friends for their never-ending support as they were an imperative support system throughout the year.

Texas A&M University strives in leadership and excellence and these are just a few core values I believe that every single person mentioned above portrays.

NOMENCLATURE

eBeam	Electron Beam
NIR	Non-ionizing Radiation
IR	Ionizing Radiation
kGy	KiloGray
PFGE	Pulsed-Field Gel Electrophoresis
TSA	Tryptic Soy Agar
TSB	Tryptic Soy Broth
CSB	Cell Suspension Buffer
SKA	Seakem Gold Agarose
CLB	Cell Lysis Buffer

CHAPTER I

INTRODUCTION

Electron Beam (eBeam) Technology

Electron beam (eBeam) technology employs ionizing radiation to ionize molecules thereby causing damaging effects in various bio-molecules. The technology relies on accelerating electrons from commercial electricity rendering them to very high energies (10 million electron volts, MeV). These highly energetic electrons are made to come in contact with materials that need to be sterilized or disinfected or their properties modified. The energetic electrons will cause structural damage to the DNA of possible microbial contaminants thereby inactivating them and rendering the product sterile. The technology is used in a wide variety of commercial applications in the medical device industry, agriculture, material sciences, and environmental industries (Pillai, 2016).

Broadly speaking there are two categories of radiation technologies: non-ionizing and ionizing radiation. The difference between the two technologies is the effect of the of energy applied. Instead of producing ionization events when passing through matter, non-ionizing radiation (NIR) has sufficient energy only for excitation. NIR is characteristic for low energy, frequency and a longer wavelength. Nevertheless, NIR is still known to cause biological effects. Few examples of NIR are infrared, microwave and radio waves that range from 10^{-6} m – 10^{2} m (Ng, 2003). On the other hand, ionizing radiation has enough energy to ionize atoms (molecules) releasing energetic electrons which will in turn interact with molecules it encounters. Few

examples of ionizing radiation are, X-rays, Gamma Rays and eBeam that have wavelength ranges of 10^{-7} m – 10^{-12} m (Figure-1).

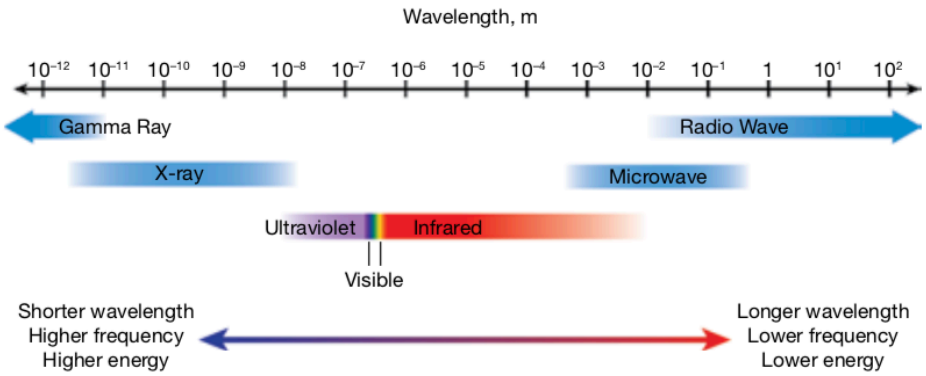

Figure-1. Electromagnetic spectrum representing ionizing and non-ionizing radiation examples (Pillai, 2016).

Although eBeam employs ionizing radiation, it differs to other IR technologies by not using radioactive materials to cause ionization events. eBeam technology accelerates electrons to almost the speed of light by a linear accelerator. These accelerators have the capacity to be turned on and off when not in use. In contrast, radioactive sources constantly emit radiation as a consequence of its natural radioactive decay. Therefore, radioactive sources cannot be "turned on and off". eBeam technology's ability to be turned on/off has major implications related to operating costs, worker safety, and carbon footprint (Pillai, 2016). The accelerated electrons are showered over and into the product (to be treated) through the eBeam horn (Figure-2). Each treatment process is calibrated in terms of absorbed dose, the amount of energy absorbed per unit mass. Kilogray (kGy) is the standard unit of absorbed dose.

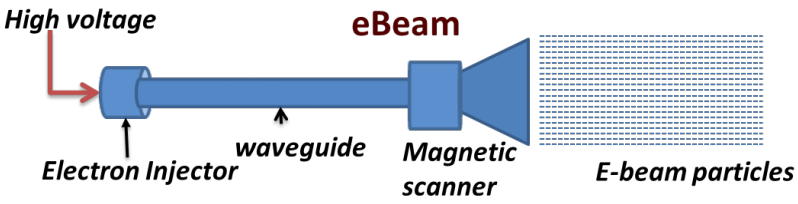

Figure-2. An eBeam linear accelerator demonstrating the direction of an electron shower (Pillai, 2016).

The target radiation dose that is delivered to a product during irradiation is controlled by the amount of time the product is held under the eBeam horn. When electrons shower the product, electrons are ejected from their orbital shells that then create a series of ionizing events (Figure-3A). When ionizing radiation encounters water molecules, hydrolysis occurs and free radicals are formed which lead to double and single strand breaks in the DNA (Figure-3B).

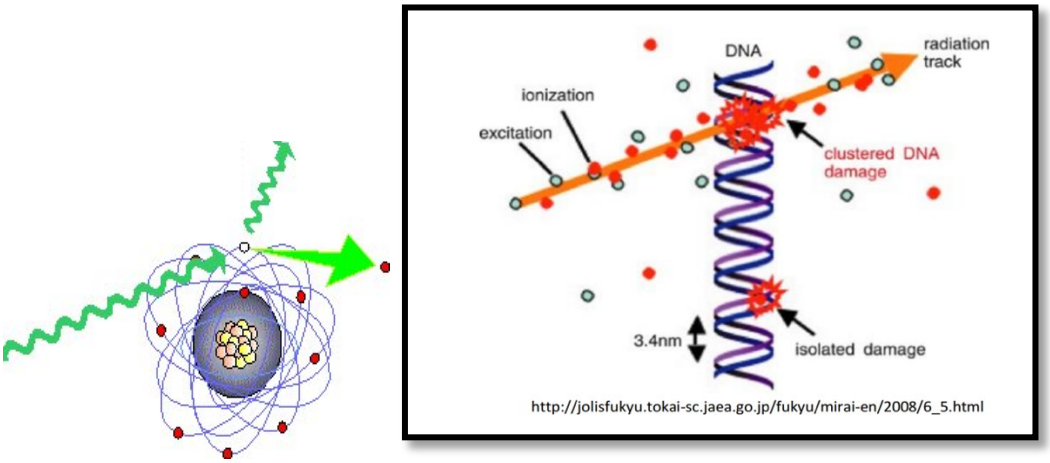

Figure-3. A) Representation of ionizing radiation knocking out an electron from its orbital shell. B) Juxtaposed double-stranded break caused by hydrolysis and reactive free radicals in DNA; thus, leading in cell inactivation (Pillai, 2016).

Even though the microbial cell has resilient repair mechanisms, the double strand breaks are so extensive leading to the halting of DNA replication; thus, inactivating the cell (Pillai, et al., 2017). Double strand breaks are the most lethal form of DNA damage because they halt DNA replication and, therefore, cellular multiplication. However, it is unclear whether there are "hot spots", or more susceptible locations in the genome for these DNA breakages. The resistance of microorganisms to ionizing radiations differ respectively, but can be compared by measuring their D-10 values. A D-10 value is defined as the dose that reduces 90% of viable microbial cells (1 $\log_{10}$ reduction) (Pillai, 2016). Therefore, processing materials with eBeam offers an opportunity to reduce viable microorganisms by defined levels. Therefore, using eBeam technology (at the appropriate eBeam dose) on a sample that has high levels of bioburden will result in a product with bioburden levels that are below detection limits.

Overall Objective

The objective of this study was to irradiate six strains of two different bacterial genera namely *E. coli* and *S. Typhimurium,* at 7kGy and 0kGy (control), to determine if DNA fragmentation occurs after eBeam irradiation and if fragmentation occurs at specific "hotspots" within the genome.

Specific Objective

1. Phase 1 involved determining whether DNA would fragment after being subjected to an eBeam dose of 7kGy. This was accomplished by using a 5200 Fragment Analyzer (Agilent, Austin, TX) to produce an electropherogram that portrayed the percent composition and concentration of fragmented bacterial DNA for non-irradiated and irradiated cells.

2. Phase 2 consisted of performing Pulse Field Gel Electrophoresis (PFGE) to determine whether fragmentation occurs at specific "hotspots" by comparing DNA fingerprints of non-irradiated and irradiated cells after being subjected for 19 hours of electrophoresis.

Rationale Behind Experimental Approach

Previous studies have shown that ionizing radiation, such as X-rays, gamma rays and eBeam, inactivates microbial cells by causing double stranded DNA breakages (Taghipour, 2004; Hieke, et. al., 2018). These double stranded breaks are created when atoms cause a series of ionizing events that lead to structural breakages (Pillai, 2018). Due to the microbial inactivation, ionizing radiation has practical uses within the medical field, water sanitation, food industry, and many more (Smathers, 1988; Husman, et. al., 2004; Pillai, 2018).

Double strand break repair has two major pathways: Homologous recombination and Non-homologous DNA End Joining (NHEJ) (Lieber, 2010). Repair enzymes within the two pathways are constantly operating until the fragment is intact once again. After eBeam exposure, it would be assumed that even these repair mechanisms would be impaired. However, recent studies in our laboratory show that the metabolism of the inactivated cell continues for extended period of time beyond the irradiation. (Bhatia and Pillai (2019). This could explain how irradiated cells, even after irradiation, are still attempting to repair their damaged (Duncan, et. al, 2018).

An aspect to consider is how these DNA breakages are occurring. Is fragmentation occurring randomly or are there specific DNA regions that are more susceptible to ionizing radiation? Oligonucleotide probing has shown how gamma ray induced mutations have occurred

at the lacI gene of *E. coli* at position 620-632, characterized by the sequence 5'-TGGC-3' (Wijker, et.al., 1996). In comparison, X-rays induce abasic clusters (loss of pyrimidine sites), oxidized pyrimidine clusters, and pyrimidine clusters (Sutherland, et. al., 2002). Research is currently occurring to better understand the effects of eBeam and to determine whether target "hotspots" exist for eBeam particles (Cauet, et. al., 2013; Keller, et. al.,2014; Reissig, et. al., 2016).

To further seek "hotspots" susceptible to eBeam, the 5200 Fragment Analyzer (Agilent, Austin, TX) could assist in determining if a pattern can be identified for microbial DNA fragmentation. Primarily, the 5200 Fragment Analyzer (Agilent, Austin, TX) offers the ability to quickly perform DNA and RNA fragmentation analysis (Agilent, 2018). The 5200 Fragment Analyzer was included in this project to evaluate percent composition and concentration of fragmented un-irradiated and irradiated bacterial DNA. The data provided the relative sizes of each bacterial DNA fragment along with the concentration for each fragment present in the sample.

For further analysis, Pulsed Field Gel Electrophoresis (PFGE) was employed to support the claim that eBeam causes DNA fragmentation. Typically, the PFGE technique is used to generate a characteristic DNA fingerprint for characterizing bacterial isolates (CDC, 2016). National and international outbreaks have been successfully identified by the use of PFGE by connecting similar cases of illness (Prager, et. al. 2003). Implementation of PFGE is a rapid (1-2days) analysis that also demonstrates genetic fingerprinting from bacterial isolates with the use of different restriction enzymes (such as XbaI, BlnI, and SpeI) to reveal fingerprint patterns and match those similar patterns to known diseases (Sandt, et. al., 2006). In these studies, PFGE was employed (without restriction endonucleases) to determine whether eBeam inactivated microbial

cells showed DNA fragmentation and whether any discernable pattern of fragmentation could be identified. PFGE allows one to visualize differences in molecular weight as a low molecular weight fragment will travel and migrate towards to bottom of the gel.

Fragment Analyzer

The Fragment Analyzer system employs a high sensitive parallel capillary electrophoresis designed to analyze dozens of DNA samples at once. The Fragment Analyzer can process up to three, 96 well plates continuously (Agilent, 2018). This technology is centered with fluorescence based parallel capillary electrophoresis requiring only one or two microliters of bacterial sample. The resolution of the Fragment Analyzer is as low as 3bp, which will be significant when measuring DNA fragments after eBeam.

Each prepared sample is voltage injected into their respective narrow capillaries arranged in a parallel orientation. The narrow capillaries contain a separation gel matrix infused with an intercalating dye used for fluorescence. Separation is achieved in electrophoresis due to the electrical field generated by the differences in charge over size ratios which allow the nucleic acid fragments in the sample to migrate based on their size (Loden, 2008). When migrating through the capillary tubes from the negatively charged buffer tray to the positively charged reservoir, the DNA fragments interact with intercalating agents and pass by a detection window. The nucleic acid bound dye is excited by an LED wavelength of 470nm; thus, producing a fluorescence emission which is detected by a CCD detector (Agilent, 2018). To quantify the size of each fragment, the CCD detector counts the time taken to navigate through the detection window. The

relative emission the fragment emits is quantified by the CCD detector to provide the nucleic acid concentration when compared to a ladder.

Once samples run through the capillary tubes, the Fragment Analyzer produces an electropherogram representing the quantities of the analyzed nucleic acid fragments. Depending on the number of peaks given in the electropherogram, the data will indicate the size and concentration within the samples.

Pulsed-Field Gel Electrophoresis

Pulsed-Field Gel Electrophoresis (PFGE) was one of the more robust technologies for comparing microbial genomes (CDC, 2018). A variation of gel electrophoresis, PFGE, can identify differences between bacterial genomes based on the level of fragmentation. In traditional PFGE analysis, restriction endonucleases are employed to cut DNA at know sequences when DNA fragments are too large (a whole genome can be used) to move throughout the gel (Parizad, et. al., 2016). However, in these studies, since the objective was to identify whether electron beam irradiation causes fragmentation of the genome we analyzed the genomes of irradiated and un-irradiated cells without the restriction endonucleases. Within PFGE, the direction of the electric field changes periodically, forcing the molecules to reorient before moving down the gel. The re-orientation allows larger and smaller molecules to separate into discrete bands in pulsed-field gels. Instead of using restriction nucleases, eBeam irradiation will be used for the experimental samples as it causes DNA fragmentation. The fragment sizes can be estimated by comparing them to a ladder and the control groups (Alberts, et. al, 2014). The motivation for this experiment was to obtain physical evidence that genome of irradiated cells is fragmented and to determine whether

the fragmentation pattern was similar within a bacterial genus. Similar fragmentation pattern within a genus would suggest that there were hot spots were DNA double strand breaks were occuring. The laboratory protocol used in these studies was based on the publicly available protocols published by the Center of Disease Control and Prevention's standard methods (CDC, website information).

CHAPTER II

METHODS

Bacterial Preparation

Six different strains of nonpathogenic *E. coli* (AM076, AM1087, 25922, DY330N, 11775, K-12) and *Salmonella Typhimurium* (13311, NVSL87-826254, 12179, MET844, SS007, PJ002) were obtained from a -80°C freezer in the Pillai laboratory culture collection.

Each strain was grown for 24 hours on a Tryptic Soy Agar (TSA) plate in a 37°C incubator. Prior to eBeam processing, an overnight culture was prepared in Tryptic Soy Broth (TSB) at 37°C for 24 hours. For each strain, a single colony was scooped from the TSA plates with previously grown stock cultures and placed into TSB media. Three biological replicates were grown for each strain. Once grown, each overnight culture was repeatedly washed three times with Phosphate Buffer Saline (PBS) solution to get rid of any residual TSB. The washing protocol was as follows: The overnight culture was centrifuged at 4000g for 10 minutes; thus, creating a bacterial pellet in the bottom of the conical tube. The supernatant was removed and 15mL of PBS was added and the solution was vortexed until the pellet was dissolved. The tubes were once again centrifuged and the steps were repeated three times. Each culture is resuspended in PBS with a final volume of 25 mL.

Electron Beam Processing

Electron beam irradiation was performed at the National Center for Electron Beam Research in College Station, TX. Before taking the bacterial samples to the eBeam processing

center, each biological replicate was aliquoted into 5mL Whirlpack bags (NASCO, Fort Atkinson, WI) and heat sealed. Each sample had to be triple bagged to avoid leaks and accidental bacterial exposure.

A control sample bag was used as the speed check. The speed check is essential to calibrate the process to achieve the targeted eBeam dose. An L- α-alanine based dosimetry system (Pravren, et. al, 2013) is used to measure eBeam doses. The dosimeters were placed appropriately (i.e., underneath the transport bags to make sure that the sample received the appropriate dose. After the samples were irradiated the dosimeters were removed and measured. Based on fine adjustments of the conveyor system based on the speed check dosimeter readings, the samples were then exposed to the eBeam irradiation at the specific calibrated conveyor belt speed to achieve the targeted dose.

Confirmation of Microbial Inactivation

After eBeam treatment, all samples were opened in a sterile environment inside a biosafety Cabinet. The triple sealed bags were cut with scissors after immerging them in ethanol and flaming the blades to ensure sterility. The samples were aliquoted into their respective containers for microbial analysis. Each undiluted container was considered as the 10^0 dilution. Ten-fold serial dilutions up to 10^{-8}, for the un-irradiated samples, were made with PBS by transferring 100uL into 900 µL dilution blanks. Dilutions were plated in TSA plates and incubated at 37°C for 24 hours. Irradiated undiluted samples were plated in TSA and incubated in the same conditions. Inactivation of microbial cultures were confirmed by lack of growth for 24 hours.

DNA Fragmentation Analysis

DNA is extracted from the un-irradiated and irradiated samples using the DNeasy Ultra Clean Microbial kit (Qiagen, Germantown, MD, as seen in Figure-4, before further downstream applications. From each undiluted sample, 1.8 mL was transferred to a 2mL collection tube and centrifuged at 10,000g for 30s. The supernatant was removed and centrifuged again at the same conditions. The remaining cell pellet was resuspended in 300 uL of PowerBead™ solution to stabilize the cell for cell lysis. The solution was transferred to a PowerBead™ tube with 50 uL of Solution SL™ that contains SDS and will breakdown fatty acids and lipids associated with the cell membrane. The solution was vortexed in a Vortex Adapter at maximum speed for 10 minutes. The tubes are centrifuged at 10,000g for 30 seconds and the supernatant was transferred to a clean tube. Before centrifuging at 10,000g for one minute, 100 uL of Solution IRS™ was added to precipitate non-DNA organic and inorganic material. The entire supernatant was transferred to a new collection tube with 900 uL of Solution SB™ to create a high salt concentration needed to bind DNA to the spin column. Once mixed, the solution was transferred into a MB Spin Column™ and centrifuged at 10,000g for 30 seconds. The flow-through is discarded and 300 uL of Solution CB™ was added and centrifuged at 10,000g for 30s to remove residues of salt and other contaminants. The column was kept and re-centrifuged for a minute to remove any residual solution CB™. The column was placed in a new collection tube and 50 uL of Solution EB™ was added to the center of the filter membrane. The tubes were then centrifuged a final time at 10,000g for 30s and DNA was released into the tube. Extracted DNA samples are stored in a -20°C freezer until needed for molecular analysis.

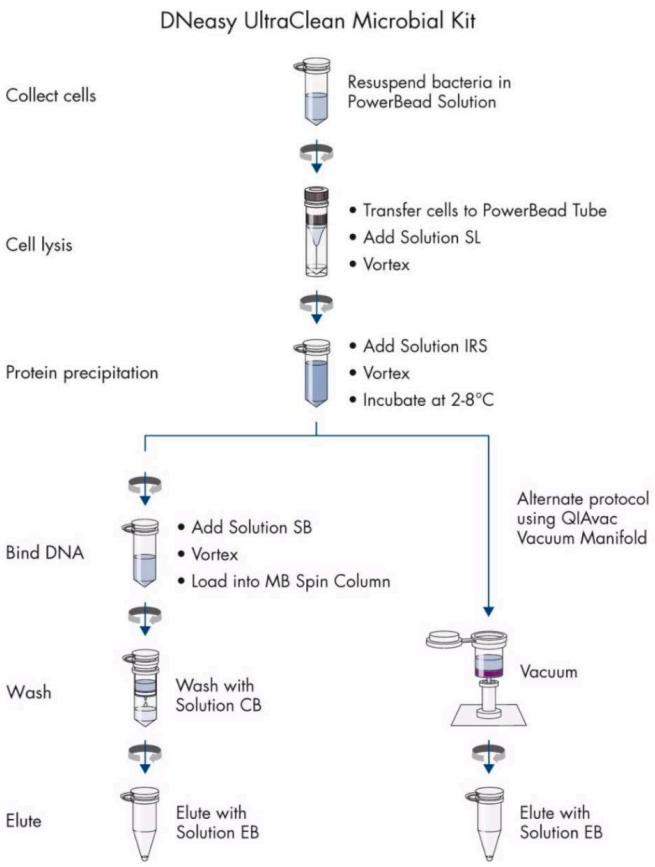

Figure-4 Qiagen Dneasy Ultra Clean Microbial synthesized protocol (Qiagen, 2017). Figure is direct reproduction from Qiagen Dneasy Ultra Clean Microbial Kit Handbook.

The DNA fragments in un-irradiated and eBeam processed samples were analyzed at the Texas A&M Genomics and Bioinformatics Center in College Station, TX. The percent composition of the differently sized fragments from un-irradiated and irradiated samples were quantified with a Fragment Analyzer software. Graphical representations were generated by the software, as seen in Appendix A. The size of the fragments in un-irradiated and irradiated cells were compared in terms of their percent composition. The fragment sizes were compared between bacterial strains and bacterial genera.

Pulsed-Field Gel Electrophoresis

After eBeam treatment, undiluted samples are ready to be cast into plugs for Pulsed-Field Gel Electrophoresis. 4.5mL of an undiluted solution was placed into 3-1.5 mL centrifuge tubes and were centrifuged at 4,000g for 10 minutes. The pellet was collected from the three replicates and were resuspended in 2mL of Cell Suspension Buffer (CSB). The solution was measured with a spectrophotometer at an OD_{600} to obtain a concentration of 0.8-1.0. This process was repeated for each bacterial strain. For the cells to undergo cell lysis, 400 uL were transferred from each solution to a new 1.5mL centrifuge tube. Mixing was done gently when adding 20 uL of Proteinase K (20mg/mL) to each tube. A reusable mold was utilized to cast the bacterial plugs. To create the plugs, 400 uL of pre-made 1% Seakem Gold Agarose (SKA) was added to the tubes and immediately transferred into the labeled plug mold. A total of three plugs were made for each biological replicate.

After the plugs solidify, they were placed into respective tubes containing a mix of 5mL of Cell Lysis Buffer (CLB) and 25 uL of Proteinase K (20mg/mL). They were left in a shaking water bath at 55°C overnight for proper cell lysis. The plugs were then washed with two rounds of 10 mL of warm sterile water and four rounds of 10mL of warm TE buffer. Between each round the tubes were shaken in a water bath for 10 minutes at 55°C. The solution was decanted and resuspended in 5mL of TE buffer and stored at 4°C until needed. Restriction enzymes were not used in this procedure. Instead of using restriction enzymes, eBeam was used to cause breakages in DNA.

Once the plugs were ready to be loaded, they were placed onto a 15 well comb and air dried for 15 minutes. Running buffer was prepared with 117.5mL of 10xTBE and 2232.5 mL of sterile water to create a 0.5X TBE solution. To cast the agarose gel, 150mL of 0.5X TBE solution was mixed with 1.5g of SKA and once the plugs were dried, the agarose was poured onto the gel casting stand with the comb inserted. Once the gel solidified, the gel was loaded onto the CHEF Mapper along with the running buffer and conditions for electrophoresis were set. Both *E. coli* and *S. Typhimurium* gels were run for 19 hours. Once the gel run was completed, the gel was stained with GelRed and an image was captured on GelDoc. The electrophoretic data was analyzed to observe differences and similarities in DNA fragment size between individual strains and between the replicate samples.

CHAPTER III

RESULTS

Confirmation of Microbial Inactivation

E. coli and *S. Typhimurium* had a starting titer of 8.98 ± 0.05 log CFU/mL and 9.28 ± 0.19 log CFU/mL, respectively. The *E. coli* samples received a measured dose of 7.47 kGy and *S. Typhimurium* received 7.02 kGy. No growth was detected in any of the irradiated samples after 24 hours on a TSA plate, confirming that irradiation achieved complete microbial inactivation.

E. coli and *S. Typhimurium* Data from Fragment Sequence Analyzer

Each sample read through the Fragment Analyzer was voltage injected into capillary tubes arranged in a parallel format. These capillaries allowed for the separation on a gel matrix infused with a fluorescent intercalating dye. Electropherograms were taken using standard Fragment Analyzer protocols from the AgriLife Genomics and Bioinformatics Center (College Station, TX). Shown in Table-1 are DNA fragment sizes, analyzed by the 5200 Fragment Analyzer (Agilent, Austin, TX), that represent how each *E. coli* strain's DNA was cut at 0 kGy and 7 kGy. Highlighted in Table-1 are the averaged sized fragments that had the highest concentration present within each biological replicate. When treated with 7 kGy, an increase of DNA shredding is visualized when comparing the highest fragment concentration between irradiated and non-irradiated samples. Shown in Table-2 are DNA fragment sizes that represent how each *S. Typhimurium* strain's DNA fragmented at 7 kGy as compared to the unirradiated cells. In Appendix A, *E. coli* and *S. Typhimurium* graphs demonstrate the pattern that each bacterial strain develops at 0kGy and at

7kGy. A similar study was done with UV irradiated products where *S. Typhimurium* samples were illustrated as 7 peaks after irradiation through capillary electrophoresis (Ozaki, et. al., 1998).

Shown in Table-1 and Table-2, there was a consistent pattern of DNA shredding within strains; although, there is none between the bacteria as a whole. Each strain exhibited similar high concentrations of DNA fragment sizes with no irradiation and at 7kGy. There is a high percent reduction between fragment sizes from control and eBeam samples. This indicates that samples irradiated with eBeam show a significant reduction in size. A similar study was done where human genomic DNA was sheared using an array of hydropores and analyzed with the fragment analyzer. The electropherogram, showed high multiple peaks describing the multiple average base pair lengths of fragments created after shearing (Lakha, et. al., 2016). The fragment analyzer cannot determine whether the DNA fragments are the same coded strands, but it does determine a commonality between fragment sizes. Irradiated samples relay common breakages within strains; thus, leading to question whether a "hotspot" exists where eBeam is more susceptible to cause damage within DNA.

Within the 0 kGy (control) column, there is fragmentation shown even in the non-irradiated samples, which shows that the DNA shearing can be expected during routine DNA extraction protocols. Mechanical shearing is natural and expected during the manual DNA extraction (Yuan, et. al., 2012). The results suggest that the majority of the fragments in the irradiated samples exhibit smaller fragment sizes as compared to the un-irradiated cells. Mechanical shearing during DNA extraction is a root for DNA cleavage; but, to justify these results, fresh samples were irradiated at the same doses and analyzed through PFGE to eliminate a mechanical cause for DNA shredding.

PFGE analysis will provide justification for DNA cleavages as the samples will be loaded onto the gel without any mechanical stress.

Table-1. DNA fragment sizes of six *E.coli* strains after 0kGy and 7 kGy treatments.

Strain AM076	**0 kGy (Control)**	**7 kGy (eBeam)**
A	**19071bp (87.7%)**	103bp (7.05%), **2304bp (90.9%)**, >60000bp (1.95%)
B	**19963bp (71.7%)**	112bp (4.81%), **2146bp (94.7%)**
C	496bp (2.38%), 4229bp (6.58%), **19591bp (65.2%),** 39372bp (8.96%)	179bp (13.2%), **2732bp (84.8%)**
Strain AM1087	**0 kGy (Control)**	**7 kGy (eBeam)**
A	88bp (0.39%), 258bp (1.04%), 496bp (8.31%), 2681bp (8.89%), **11998bp (79.7%)**, >6000bp (0.41%)	102bp (13.6%), **5081bp (90.6%)**, >60000bp (0.21%)
B	581bp (5.11%), 2768bp (12.4%), **19172bp (61.0%),** 35960bp (4.92%)	106bp (1.34%), **4636bp (98.2%)**
C	**22145bp (66.7%)**	98bp (1.25%), **5709bp (89.3%),** 58984bp (0.31%)
Strain 25922	**0 kGy (Control)**	**7 kGy (eBeam)**
A	83bp (0.64%), 541bp (1.70%), 694bp (0.67%), 1120bp (1.01%), **14636bp (92.2%)**	201bp (10.9%), **4609bp (84.9%)**
B	95bp (2.2%), 262bp (4.05%), 532bp (3.21%), 731bp (1.86%), 1143bp (1.93%), **12938bp (83.6%)**	196bp (14.5%), **4672bp (75.6%)**
C	92bp (1.84%), 264bp (3.74%), 580bp (4.13%), 1094bp (2.17%), **13213bp (83.1%),** >60000bp (0.001%)	212bp (24.0%), **3917bp (65.5%)**
Strain DY330N	**0 kGy (Control)**	**7 kGy (eBeam)**
A	**20173bp (81.0%)**	**9356bp (70.4%)**
B	**18434bp (73.5%)**	**11002bp (58.6%)**
C	491bp (2.19%), **19369bp (85.6%)**	257bp (3.36%), **10177bp (75.5%)**
Strain 11775	**0 kGy (Control)**	**7 kGy (eBeam)**
A	83bp (0.70%), 348bp (2.05%), **14679bp (96.0%)**	**9226bp (78.8%)**
B	463bp (2.38%), **13874bp (96.3%)**, 40629bp (0.24%), >60000bp (0.22%)	**8636bp (79.7%)**, >60000bp (1.10%)
C	88bp (0.33%), 457bp (2.52%), **15063bp (95.2%),** >60000bp (0.74%)	**8437bp (80.6%)**
Strain K-12	**0 kGy (Control)**	**7 kGy (eBeam)**
A	133bp (0.48%), 267bp (0.14%), 468bp (2.41%), **12151bp (95.2%),** 39576bp (0.23%), >60000bp (0.83%)	159bp (2.80%), **9412bp (92.2%)**
B	484bp (2.39%), **18467bp (96.1%)**	172bp (3.94%), **9009bp (92.2%)**, >60000bp (0.41%)
C	461bp (1.90%), **14477bp (96.8%),** >60000bp (0.17%)	152bp (3.11%), 791bp (3.12%), **9829bp (90.0%),** >60000bp (1.44%)

Table-2. DNA fragment sizes of six *S. Typhimurium* strains after 0kGy and 7 kGy treatments.

Strain 13311	**0 kGy (Control)**	**7 kGy (eBeam)**
A	88bp (0.90%), 275bp (0.85%), 434bp (1.96%), 558bp (1.98%), **9719bp (94.2%)**	**160bp (40.9%)**
B	**27614bp (99.1%)**	**99bp (65.0%)**
C	282bp (0.38%), 444bp (1.56%), 576bp (1.88%), **14597bp (94.5%)**	**99bp (67.8%)**
Strain NVSL87-826254	**0 kGy (Control)**	**7 kGy (eBeam)**
A	71bp (3.70%), 280bp (2.24%), 394bp (4.28%), 567bp (1.16%), **9672bp (88.5%)**	**9346bp (90.5%)**
B	**23827bp (89.8%)**, >60000bp (3.93%)	**9836bp (80.3%)**
C	**17624bp (89.5%),** >60000bp (3.36%)	**12158bp (80.7%)**
Strain 12179	**0 kGy (Control)**	**7 kGy (eBeam)**
A	**18812bp (84.9%)**	**9346bp (88.2%)**
B	**17921bp (98.5%)**	103bp (0.61%), **9807bp (96.9%)**
C	309bp (6.46%), **19901bp (74.4%)**	**13535bp (91.4%)**
Strain MET844	**0 kGy (Control)**	**7 kGy (eBeam)**
A	72bp (1.81%), 269bp (1.20%), 437bp (4.41%), 532bp (0.89%), **9953bp (90.5%)**	**16293bp (96.1%)**
B	**21570bp (88.0%)**	**15000bp (96.3%)**
C	73bp (0.09%), 279bp (0.87%), 459bp (4.54%), 569bp (0.97%), **12581bp (90.7%),** 37699bp (0.60%)	**15656bp (97.1%)**
Strain SS007	**0 kGy (Control)**	**7 kGy (eBeam)**
A	**13862bp (85.5%)**	388bp (5.57%)**, 3941bp (93.8%)**
B	**16238bp (88.9%)**	**9420bp (92.0%)**
C	450bp (6.47%), **15000bp (88.9%)**	**10260bp (95.8%)**
Strain PJ002	**0 kGy (Control)**	**7 kGy (eBeam)**
A	**16733bp (87.8%)**	**9952bp (92.8%)**
B	**15644bp (80.0%)**	**11122bp (89.1%)**
C	**17822bp (96.8%)**	**10432bp (89.2%)**

E. coli and *S. Typhimurium* Data from Pulsed-Field Gel Electrophoresis

Pulsed Field Gel Electrophoresis was used to reduce the amount of mechanical shredding that could occur during DNA extraction. Pulse Field Gel Electrophoresis allows separation of complete genomes within a sample (CDC, 2018). Within PFGE, depending on the size of the

genome that was analyzed, restriction nucleases select for certain sequences to allow for proper sorting. Instead of using restriction nucleases, eBeam irradiation was used for the experimental samples as it causes double strand breakages within DNA. Appendix B illustrates a series of images depicted after staining each gel with Gel Red. Each gel contains irradiated and non-irradiated samples of the same bacterial strain. Within each gel there are two replicates of the same biological replicate.

The first half of the gel (wells 1-8) show a straight comparison between 0kGy and 7kGy and the second half of the gel (wells 9-15) shows comparison between biological strains with the same targeted dose. Non-irradiated samples exhibit a smear located at the top part of the gel. As seen in Appendix B, fragments located at the top part of the gel represent those with a higher molecular weight. Each image of the gel has an un-irradiated and irradiated fragment encased in a green circle to compare how un-irradiated samples have bands at a higher molecular weight, but are not present within the irradiated samples. The PFGE pattern from the irradiated samples exhibit a smear at the lower part of the gel. Each image of the gel has a blue circle encasing multiple fragments illustrating lower molecular weights in eBeam treated and un-irradiated cells. A comparison between samples show how only eBeam treated cells gather at the lower end of the gel due to their lower molecular fragments. There is no clear band pattering, due to the numerous fragment sizes created after PFGE, but the smears at the lower part of the gel show how eBeam causes DNA breakages after irradiation. A previous study illustrates a PFGE gel with human dermal fibroblast cells after X-ray irradiation at different doses. DNA from the irradiated cells decrease in smear size and appear at the bottom part of the gel (Löbrich, 1995).

In Pulsed Field Gel Electrophoresis, the rate the samples travel across the gel depends on the molecular size of the fragments. The smaller the fragment, the faster it will travel across the gel. The gels relate a pattern specific to their respective biological replicate, but it is not clear whether these breakages were random or targeted at a specific location. The gels showed high expression in certain areas where similar sized fragments are concentrated. The following steps are to sequence several parts of a PFGE gel and after DNA extraction to determine what sequences are located within the fragmented segments.

CHAPTER IV

CONCLUSION

Electron beam (eBeam) technology is known to cause double stranded breaks in microbial cells (Taghipour, 2004; Hieke, et. al., 2018). These double stranded breaks if extensive and juxtaposed from each other will prevent DNA replication and prevent multiplication of cells and thereby inactivating the cells (Pillai, 2016). In order to confirm this claim, six different strains of *E. coli* and *S. Typhimurium* were subjected to a kill dose of 7 kGy. DNA was extracted from each sample and analyzed by a DNA fragment analyzer and by Pulsed Field Gel Electrophoresis.

Experimental data from the Fragment Analyzer suggests that eBeam does cause fragmentation of the genomic DNA. When electropherograms were compared between irradiated specific strains, fragments had similar base pair sizes between the biological replicates. Each biological replicate was treated as its own sample and after irradiation, the results show a similar pattern between them. Although there were traces of natural mechanical shearing, irradiated and non-irradiated samples fragment at sizes proximal to each replicate. This suggests that eBeam-irradiated samples have a similar DNA fragmentation pattern when subjected to a dose of 7kGy.

Data from Pulse Field Gel Electrophoresis suggest that genomic DNA from the irradiated cells, compared to un-irradiated cells, travel at a faster rate towards the bottom of the gel due to the fragment's low molecular weight. This suggests that when microbial cells are exposed to lethal eBeam doses, the DNA gets fragmented as a result of extensive double-strand breakages. Overall

data from the PFGE suggests that bacterial cells fragment when the samples were subjected to a dose of 7kGy.

These studies provide strong evidence that when exposed to lethal eBeam doses, bacterial DNA is fragmented. This can be seen in both the results from the Fragment Analyzer and from the PFGE. However, the results are inconclusive as to whether there are “hot spots” where double stranded DNA breaks occur when subjected to ionizing radiation such as eBeam. More effort is needed to design studies that will provide an insight as to whether “hot spots” occur on bacterial genomes.

REFERENCES

Agilent, *Reliable Results for Nucleic Acid Analysis Agilent 5200, 5300, and 5400 Fragment Analyzer Systems*. (2018). Retrieved from https://www.aati-us.com/documents/brochures/Fragment Analyzer Brochure.pdf

Agilent *Fragment Analyzer Automated CE System*. (2018). Retrieved from www.agilent.com/chem/contactus

Alberts, B., Johnson, A., & Lewis, J. (2014). *Molecular Biology of the Cell* (6th ed.). New York, NY: Garland Science Taylor & Francis.

Anazawa, T., Takahashi, S., & Kambara, H. (1996). A Capillary Array Gel Electrophoresis System Using Multiple Laser Focusing for DNA Sequencing. *Analytical Chemistry*, *68*(15), 2699–2704. https://doi.org/10.1021/ac9601831

Bhatia, S. S., & Pillai, S. D. (2019). A Comparative Analysis of the Metabolomic Response of Electron Beam Inactivated E. coli O26:H11 and Salmonella Typhimurium ATCC 13311. *Frontiers in Microbiology*, *10*, 694. https://doi.org/10.3389/fmicb.2019.00694

Cauët, E., Bogatko, S., Liévin, J., De Proft, F., & Geerlings, P. (2013). Electron-Attachment-Induced DNA Damage: Instantaneous Strand Breaks. *The Journal of Physical Chemistry B*, *117*(33), 9669–9676. https://doi.org/10.1021/jp406320g

CDC. (2018). *STANDARD OPERATING PROCEDURE FOR PULSENET PFGE OF ESCHERICHIA COLI O157:H7, ESCHERICHIA COLI NON-O157 (STEC), SALMONELLA SEROTYPES, SHIGELLA SONNEI AND SHIGELLA FLEXNERI*. Retrieved from https://www.cdc.gov/pulsenet/pdf/ecoli-shigella-salmonella-pfge-protocol-508c.pdf

CDC. (2016). Pulsed-field Gel Electrophoresis (PFGE) | PulseNet Methods| PulseNet | CDC. Retrieved April 11, 2019, from https://www.cdc.gov/pulsenet/pathogens/pfge.html

De Roda Husman, A. M., Bijkerk, P., Lodder, W., Van Den Berg, H., Pribil, W., Cabaj, A., … Duizer, E. (2004). Calicivirus inactivation by nonionizing (253.7-nanometer-wavelength [UV]) and ionizing (gamma) radiation. *Applied and Environmental Microbiology*, *70*(9), 5089–5093. https://doi.org/10.1128/AEM.70.9.5089-5093.2004

Duncan, J. R., Lieber, M. R., Adachi, N., & Wahl, R. L. (2018). DNA Repair After Exposure to Ionizing Radiation Is Not Error-Free. *Journal of Nuclear Medicine: Official Publication, Society of Nuclear Medicine*, *59*(2), 348. https://doi.org/10.2967/jnumed.117.197673

Ejrnaes, K., Sandvang, D., Lundgren, B., Ferry, S., Holm, S., Monsen, T., … Frimodt-Moller, N. (2006). Pulsed-field gel electrophoresis typing of Escherichia coli strains from samples collected before and after pivmecillinam or placebo treatment of uncomplicated community-acquired urinary tract infection in women. *Journal of Clinical Microbiology*, *44*(5), 1776–1781. https://doi.org/10.1128/JCM.44.5.1776-1781.2006

Herskovits, A. A., Giedlin, M. A., Stassinopoulos, A., Gao, Y., Luckett, W., Schnupf, P., … Hearst, J. E. (2005). Killed but metabolically active microbes: a new vaccine paradigm for eliciting effector T-cell responses and protective immunity. *Nature Medicine*, *11*(8), 853–860. https://doi.org/10.1038/nm1276

Hieke, A.-S. C., & Pillai, S. D. (2018). Escherichia coli Cells Exposed to Lethal Doses of Electron Beam Irradiation Retain Their Ability to Propagate Bacteriophages and Are Metabolically Active. *Frontiers in Microbiology*, *9*, 2138. https://doi.org/10.3389/fmicb.2018.02138

Huang, X. C., Quesada, M. A., & Mathies, R. A. (1992). DNA sequencing using capillary array electrophoresis. *Analytical Chemistry*, *64*(18), 2149–2154. https://doi.org/10.1021/ac00042a021

Huang, X. C., Quesada, M. A., & Mathies, R. A. (1992). Capillary array electrophoresis using laser-excited confocal fluorescence detection. *Analytical Chemistry*, *64*(8), 967–972. https://doi.org/10.1021/ac00032a025

Hutchinson, F. (1985). Chemical Changes Induced in DNA by Ionizing Radiation. *Progress in Nucleic Acid Research and Molecular Biology*, *32*, 115–154. https://doi.org/10.1016/S0079-6603(08)60347-5

Keller, A., Rackwitz, J., Cauët, E., Liévin, J., Körzdörfer, T., Rotaru, A., … Bald, I. (2015). Sequence dependence of electron-induced DNA strand breakage revealed by DNA nanoarrays. *Scientific Reports*, *4*(1), 7391. https://doi.org/10.1038/srep07391

Kempner, E. S. (2001). Effects of high-energy electrons and gamma rays directly on protein molecules. *Journal of Pharmaceutical Sciences*, *90*(10), 1637–1646. Retrieved from http://www.ncbi.nlm.nih.gov/pubmed/11745722

Khan, S. R., & Kuzminov, A. (2017). Pulsed-field gel electrophoresis does not break E. coli chromosome undergoing excision repair after UV irradiation. *Analytical Biochemistry*, *526*, 66–68. https://doi.org/10.1016/j.ab.2017.03.019

Lakha, W., Panteleeva, I., Squazzo, S., Saxena, R., Kroonen, J., Siembieda, S., … Hagopian, J. (2016). DNA fragmentation and quality control analysis using Diagenode shearing systems and Fragment Analyzer. *Nature Methods*, *13*(10), iii–iv. https://doi.org/10.1038/nmeth.f.397

Lieber, M. R. (2010). The mechanism of double-strand DNA break repair by the nonhomologous DNA end-joining pathway. *Annual Review of Biochemistry*, *79*, 181–211. https://doi.org/10.1146/annurev.biochem.052308.093131

Löbrich, M., Rydberg, B., & Cooper, P. K. (1995). Repair of x-ray-induced DNA double-strand breaks in specific Not I restriction fragments in human fibroblasts: joining of correct and incorrect ends. *Proceedings of the National Academy of Sciences of the United States of*

America, *92*(26), 12050–12054. Retrieved from http://www.ncbi.nlm.nih.gov/pubmed/8618842

Lodén, H. (2008). *Separation of pharmaceuticals by capillary Electrophoresis using partial filling and multiple-injections*. Acta Universitatis Upsaliensis. Retrieved from https://www.researchgate.net/publication/265578449_Separation_of_Pharmaceuticals_by_Capillary_Electrophoresis_using_Partial_Filling_and_Multiple-injections

Mathies, R. A., & Huang, X. C. (1992). Capillary array electrophoresis: an approach to high-speed, high-throughput DNA sequencing. *Nature*, *359*(6391), 167–169. https://doi.org/10.1038/359167a0

Meißner, R., Makurat, S., Kozak, W., Limão-Vieira, P., Rak, J., & Denifl, S. (2019). Electron-Induced Dissociation of the Potential Radiosensitizer 5-Selenocyanato-2′-deoxyuridine. *The Journal of Physical Chemistry B*, *123*(6), 1274–1282. https://doi.org/10.1021/acs.jpcb.8b11523

Moawed, F. S., El-Sonbaty, S. M., & Mansour, S. Z. (2019). Gallium nanoparticles along with low-dose gamma radiation modulate TGF-β/MMP-9 expression in hepatocellular carcinogenesis in rats. *Tumor Biology*, *41*(3), 101042831983485. https://doi.org/10.1177/1010428319834856

Ng, K.-H. (2013). *Non-Ionizing Radiations-Sources, Biological Effects, Emissions and Exposures*. Retrieved from https://www.who.int/peh-emf/meetings/archive/en/keynote3ng.pdf

Nguyen, V., Panyutin, I. V., Panyutin, I. G., & Neumann, R. D. (2016). A Genomic Study of DNA Alteration Events Caused by Ionizing Radiation in Human Embryonic Stem Cells via Next-Generation Sequencing. *Stem Cells International*, *2016*, 1–7. https://doi.org/10.1155/2016/1346521

Ohadian Moghadam, S., Pourmand, M. R., Douraghi, M., Sabzi, S., & Ghaffari, P. (2017). Utilization of PFGE as a Powerful Discriminative Tool for the Investigation of Genetic Diversity among MRSA Strains. *Iranian Journal of Public Health*, *46*(3), 351–356. Retrieved from http://www.ncbi.nlm.nih.gov/pubmed/28435821

Ozaki, A., Kitano, M., Itoh, N., Kuroda, K., Furusawa, N., Masuda, T., & Yamaguchi, H. (1998). Mutagenicity and DNA-damaging Activity of Decomposed Products of Food Colours under UV irradiation. *Food and Chemical Toxicology*, *36*(9–10), 811–817. https://doi.org/10.1016/S0278-6915(98)00039-8

Parizad, E. G., Parizad, E. G., & Valizadeh, A. (2016). The Application of Pulsed Field Gel Electrophoresis in Clinical Studies. *Journal of Clinical and Diagnostic Research: JCDR*, *10*(1), DE01-4. https://doi.org/10.7860/JCDR/2016/15718.7043

Pasternak, C., Ton-Hoang, B., Coste, G., Bailone, A., Chandler, M., & Sommer, S. (2010). Irradiation-Induced Deinococcus radiodurans Genome Fragmentation Triggers Transposition of a Single Resident Insertion Sequence. *PLoS Genetics*, *6*(1), e1000799. https://doi.org/10.1371/journal.pgen.1000799

Pillai, S. D. (2016). Introduction to Electron-Beam Food Irradiation. *Chemical Engineering Progress*, *112*(11), 36–44.

Pillai, S. D., & Shayanfar, S. (2017). Electron Beam Technology and Other Irradiation Technology Applications in the Food Industry. *Topics in Current Chemistry*. https://doi.org/10.1007/s41061-016-0093-4

Prager, R., & Tschäpe, H. (n.d.). [Genetic fingerprinting (PFGE) of bacterial isolates for their molecular epidemiology]. *Berliner Und Munchener Tierarztliche Wochenschrift*, *116*(11–12), 474–481. Retrieved from http://www.ncbi.nlm.nih.gov/pubmed/14655625

Praveen, C., Jesudhasan P.R., Reimers, R., Pillai, S., *Electron beam inactivation of selected microbial pathogens and indicator organisms in aerobically and anaerobically digested sewage sludge*, Bioresource Technology, Volume 144, September 2013, Pages 652-657.

Qiagen, *Dneasy Ultra Clean Microbial Kit Handbook*. (2017). Retrieved from https://www.qiagen.com/us/resources/resourcedetail?id=26d8d1f5-6aab-495e-931b-55a3b3c5ec36&lang=en

Radman, M. (2016). Protein damage, radiation sensitivity and aging. *DNA Repair*, *44*, 186–192. https://doi.org/10.1016/j.dnarep.2016.05.025

Reissig, F., Mamat, C., Steinbach, J., Pietzsch, H.-J., Freudenberg, R., Navarro-Retamal, C., … Wunderlich, G. (2016). Direct and Auger Electron-Induced, Single- and Double-Strand Breaks on Plasmid DNA Caused by 99mTc-Labeled Pyrene Derivatives and the Effect of Bonding Distance. *PLOS ONE*, *11*(9), e0161973. https://doi.org/10.1371/journal.pone.0161973

Sandt, C. H., Krouse, D. A., Cook, C. R., Hackman, A. L., Chmielecki, W. A., & Warren, N. G. (2006). The key role of pulsed-field gel electrophoresis in investigation of a large multiserotype and multistate food-borne outbreak of Salmonella infections centered in Pennsylvania. *Journal of Clinical Microbiology*, *44*(9), 3208–3212. https://doi.org/10.1128/JCM.01404-06

Smathers, J. B. (1988). Uses of ionizing radiation and medical-care-related problems. *Health Physics*, *55*(2), 165–167. Retrieved from http://www.ncbi.nlm.nih.gov/pubmed/3137187

Sutherland, B. M., Bennett, P. V, Sutherland, J. C., & Laval, J. (2002). Clustered DNA damages induced by x rays in human cells. *Radiation Research*, *157*(6), 611–616. Retrieved from http://www.ncbi.nlm.nih.gov/pubmed/12005538

Taghipour, F. (2004). Ultraviolet and ionizing radiation for microorganism inactivation. *Water Research*, *38*(18), 3940–3948. https://doi.org/10.1016/j.watres.2004.06.016

Tan, S. C., & Yiap, B. C. (2009). DNA, RNA, and protein extraction: the past and the present. *Journal of Biomedicine & Biotechnology*, *2009*, 574398. https://doi.org/10.1155/2009/574398

Tchurikov, N. A., Yudkin, D. V, Gorbacheva, M. A., Kulemzina, A. I., Grischenko, I. V, Fedoseeva, D. M., … Kretova, O. V. (2016). Hot spots of DNA double-strand breaks in human rDNA units are produced in vivo. *Scientific Reports*, *6*, 25866. https://doi.org/10.1038/srep25866

Wijker, C. A., Lafleur, M. V, van Steeg, H., Mohn, G. R., & Retèl, J. (1996). Gamma-radiation-induced mutation spectrum in the episomal lacI gene of Escherichia coli under oxic conditions. *Mutation Research*, *349*(2), 229–239. Retrieved from http://www.ncbi.nlm.nih.gov/pubmed/8600354

Wagner, K., Springer, B., Pires, V. P., & Keller, P. M. (2019). High-throughput screening of bacterial pathogens in clinical specimens using 16S rDNA qPCR and fragment analysis. *Diagnostic Microbiology and Infectious Disease*, *93*(4), 287–292. https://doi.org/10.1016/J.DIAGMICROBIO.2018.11.006

Yuan, S., Cohen, D. B., Ravel, J., Abdo, Z., & Forney, L. J. (2012). Evaluation of Methods for the Extraction and Purification of DNA from the Human Microbiome. *PLoS ONE*, *7*(3), e33865. https://doi.org/10.1371/journal.pone.0033865

Yushkova, E., & Zainullin, V. (n.d.). [Radiation-induced DNA fragmentation in cells of somatic and generative tissues of Drosophila melanogaster]. *Radiatsionnaia Biologiia, Radioecologiia*, *55*(1), 97–103. Retrieved from http://www.ncbi.nlm.nih.gov/pubmed/25962282

Zagorski, Z. P. (n.d.). *XA0055122 THIN LAYER ALANINE DOSIMETER WITH OPTICAL SPECTROPHOTOMETRIC EVALUATION*. Retrieved from https://inis.iaea.org/collection/NCLCollectionStore/_Public/31/035/31035843.pdf?r=1&r=1

Zhou, D. D., Hao, J. L., Guo, K. M., Lu, C. W., & Liu, X. D. (2016). Sperm quality and DNA damage in men from Jilin Province, China, who are occupationally exposed to ionizing radiation. *Genetics and Molecular Research*, *15*(1). https://doi.org/10.4238/gmr.15018078

APPENDIX A

1A0	1A7
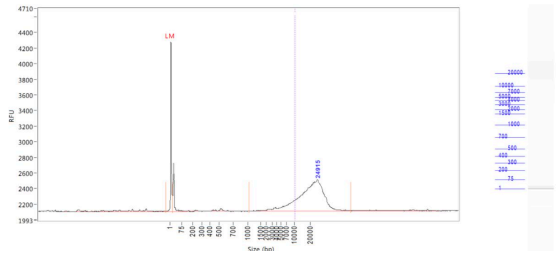	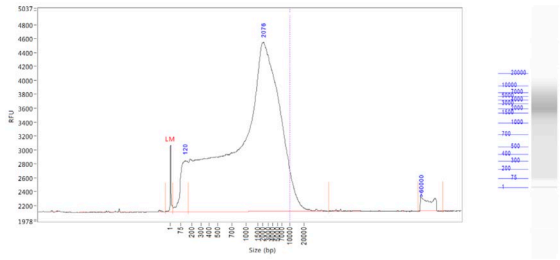
1B0	**1B7**
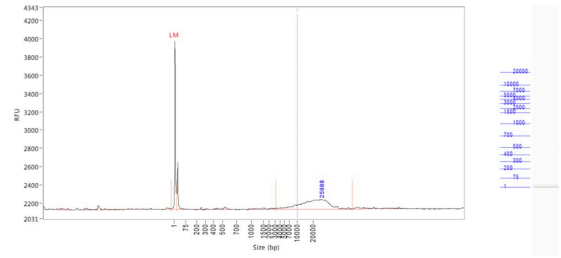	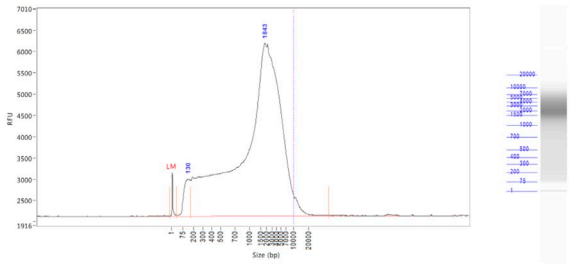
1C0	**1C7**
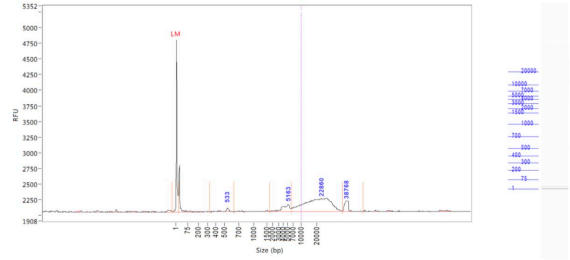	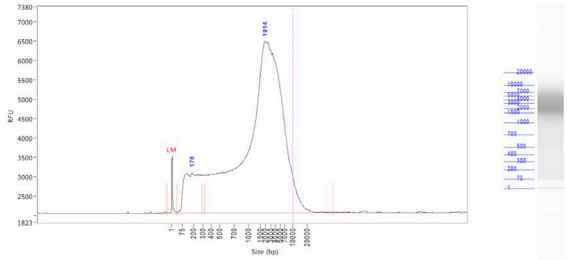

Figure-5: *E. coli* AM076 Fragment Analyzer Data

2A0	2A7
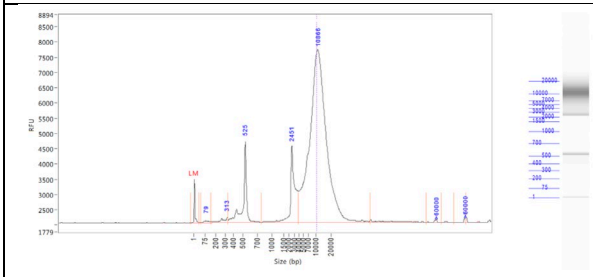	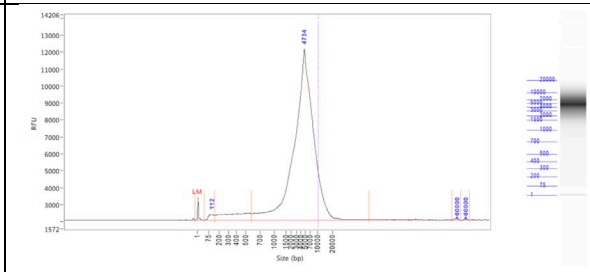
2B0	**2B7**
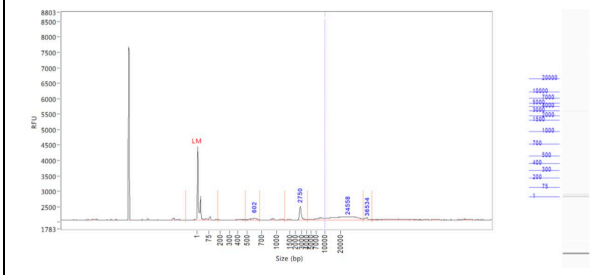	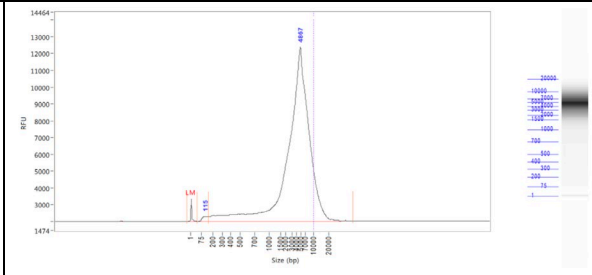
2C0	**2C7**
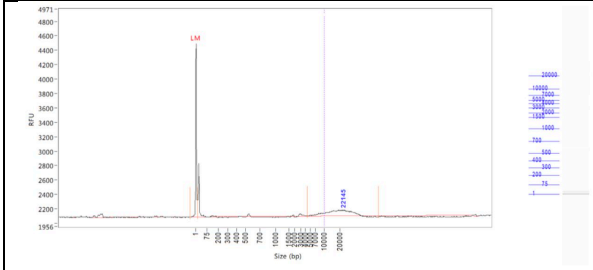	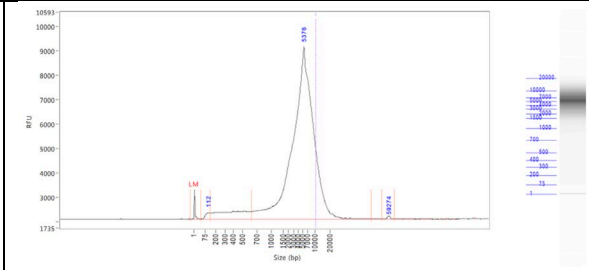

Figure-6: *E. coli* AM1087 Fragment Analyzer Data

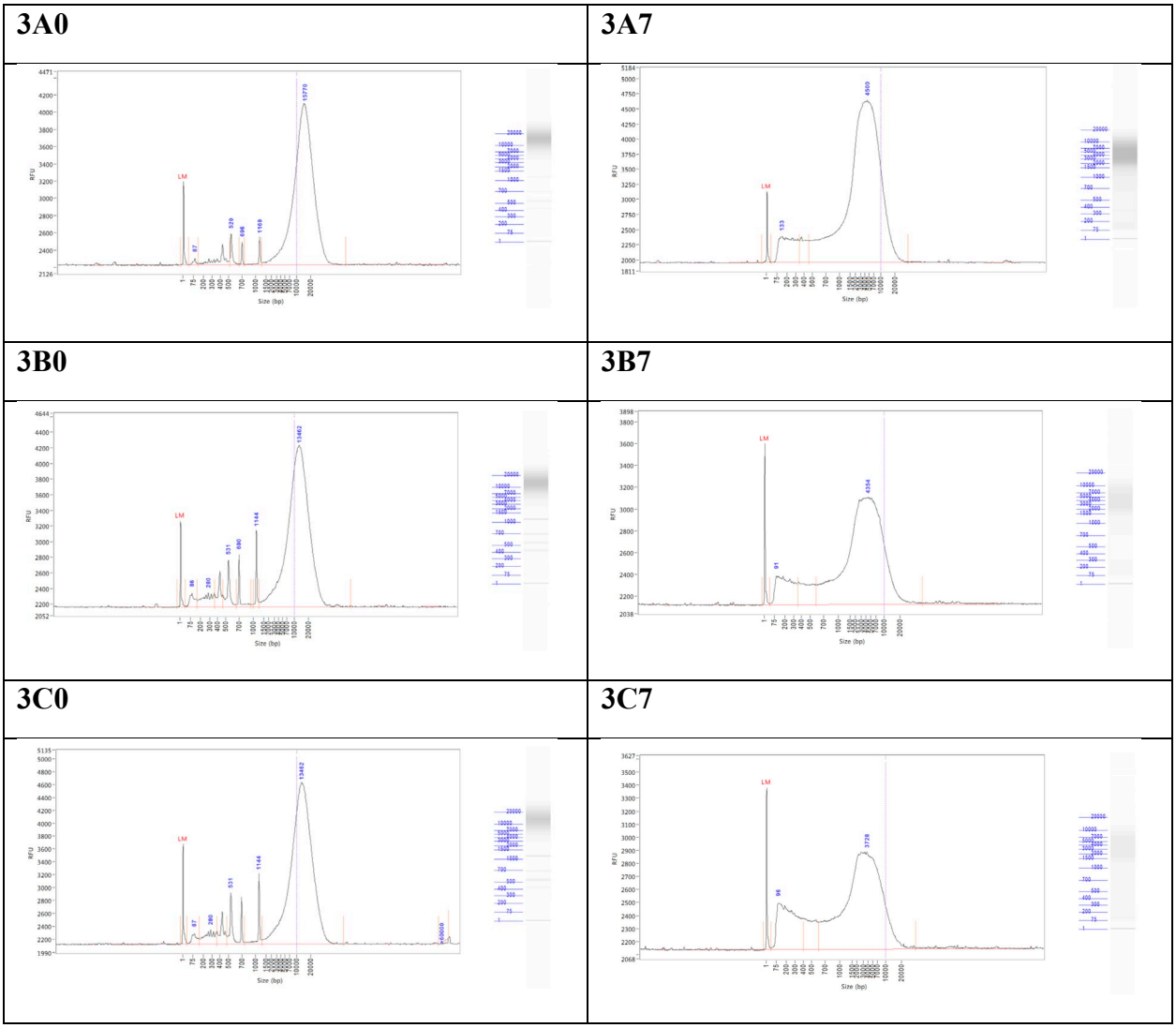

Figure-7: *E. coli* 25922 Fragment Analyzer Data

4A0	4A7
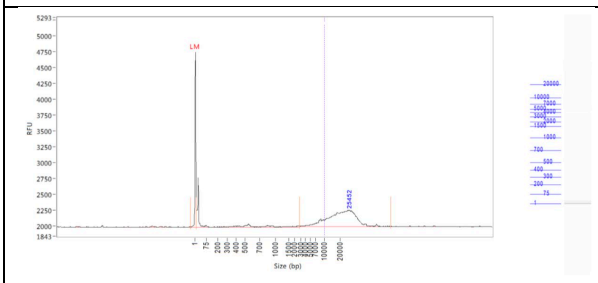	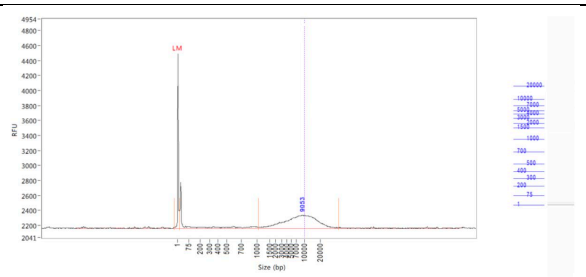
4B0	**4B7**
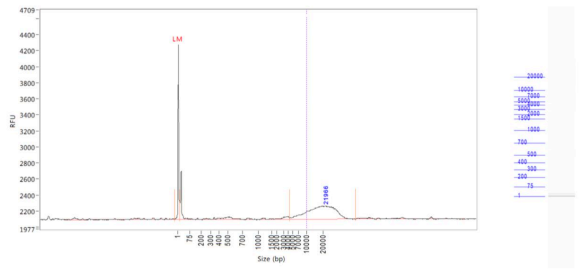	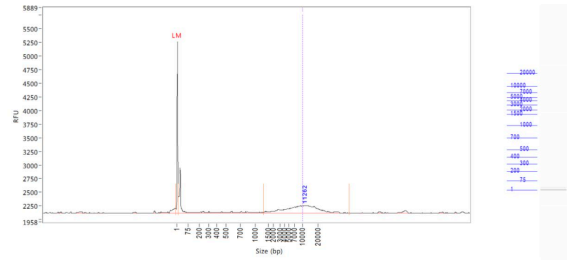
4C0	**4C7**
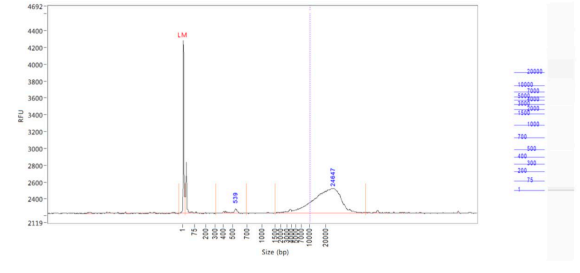	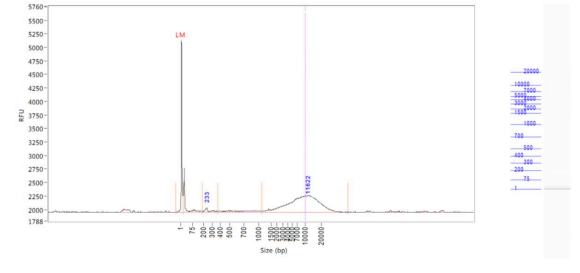

Figure-8: *E. coli* DY330N Fragment Analyzer Data

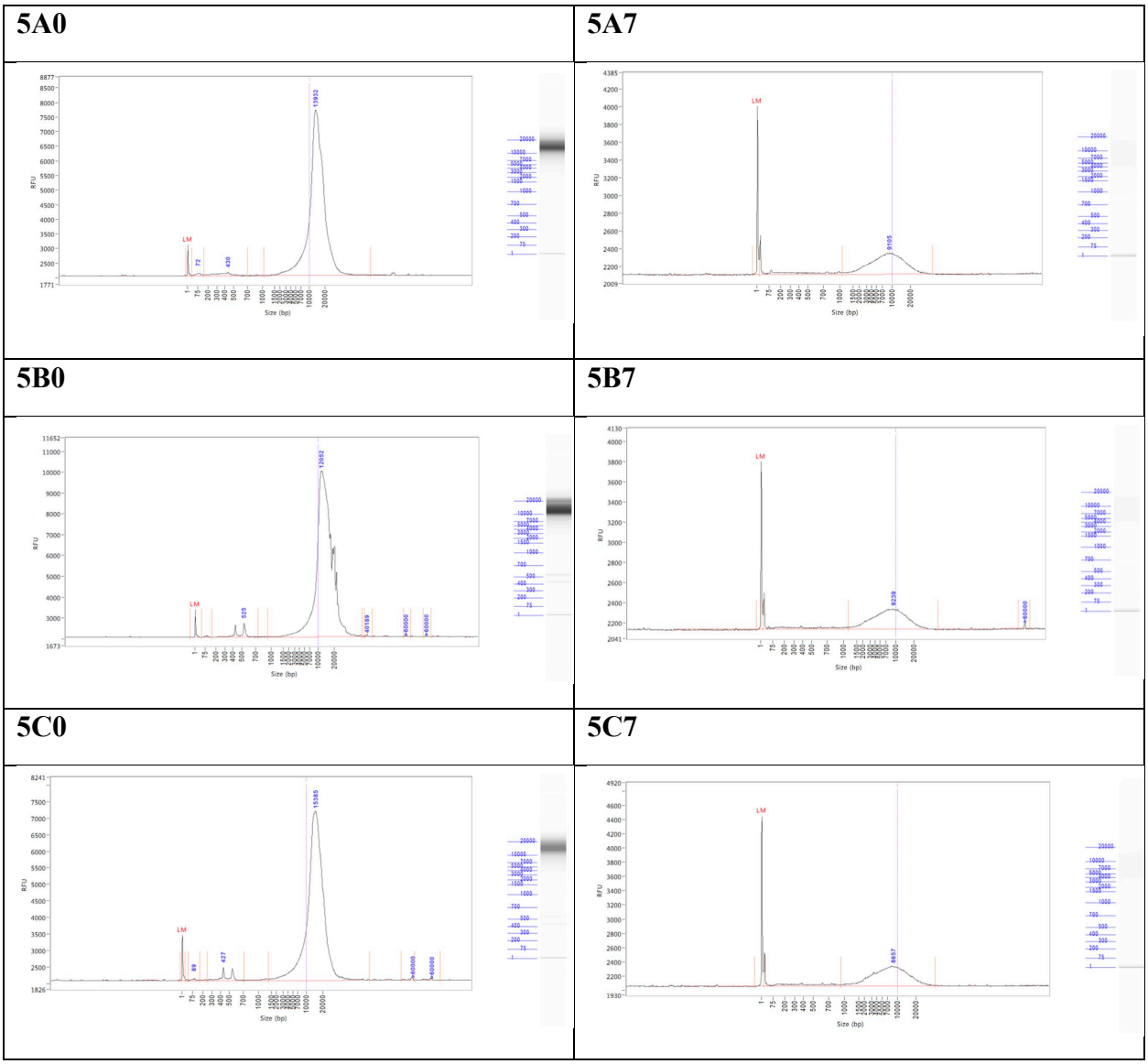

Figure- 9: *E. coli* 117755 Fragment Analyzer Data

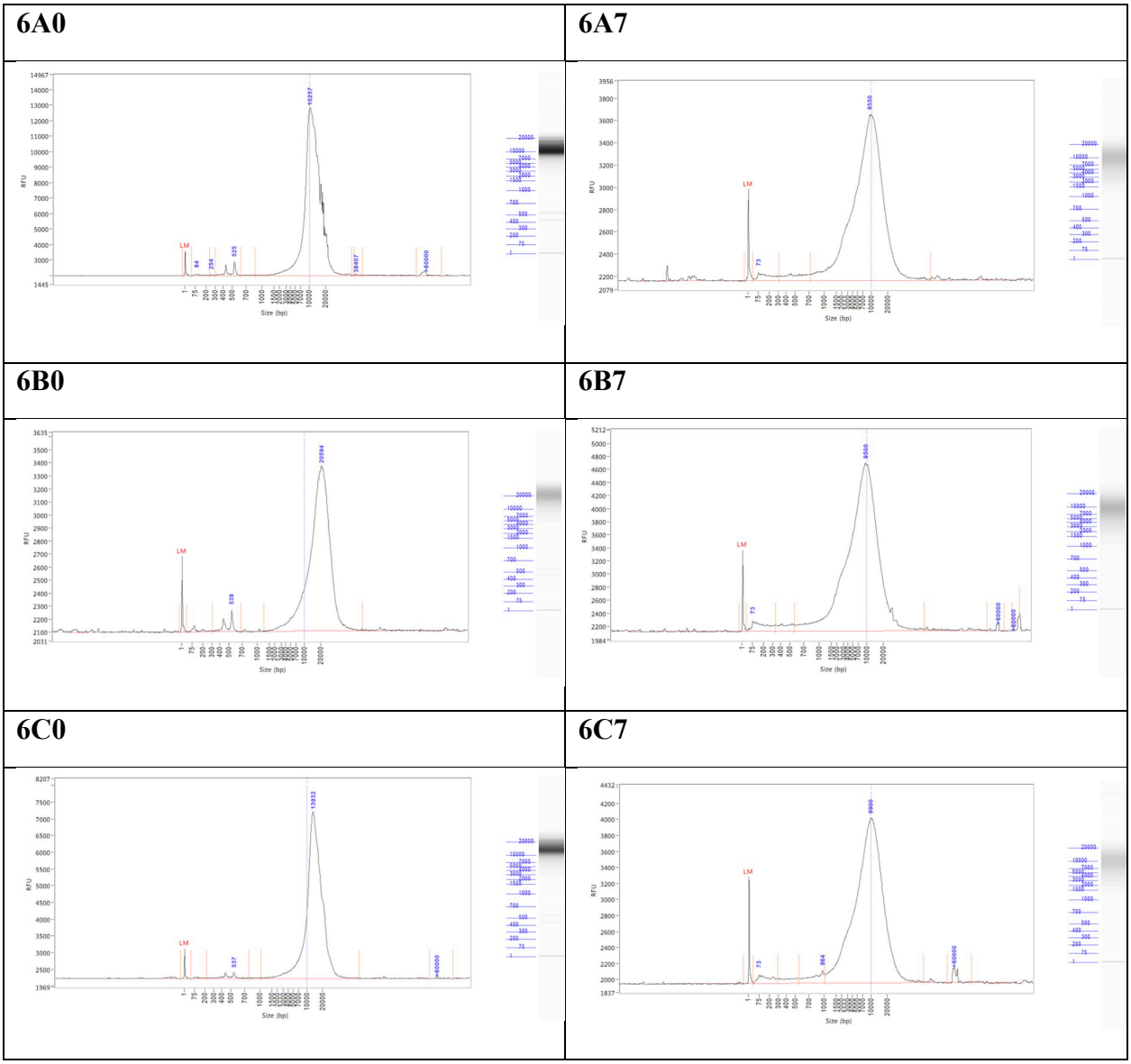

Figure-10: *E. coli* K-12 Fragment Analyzer Data

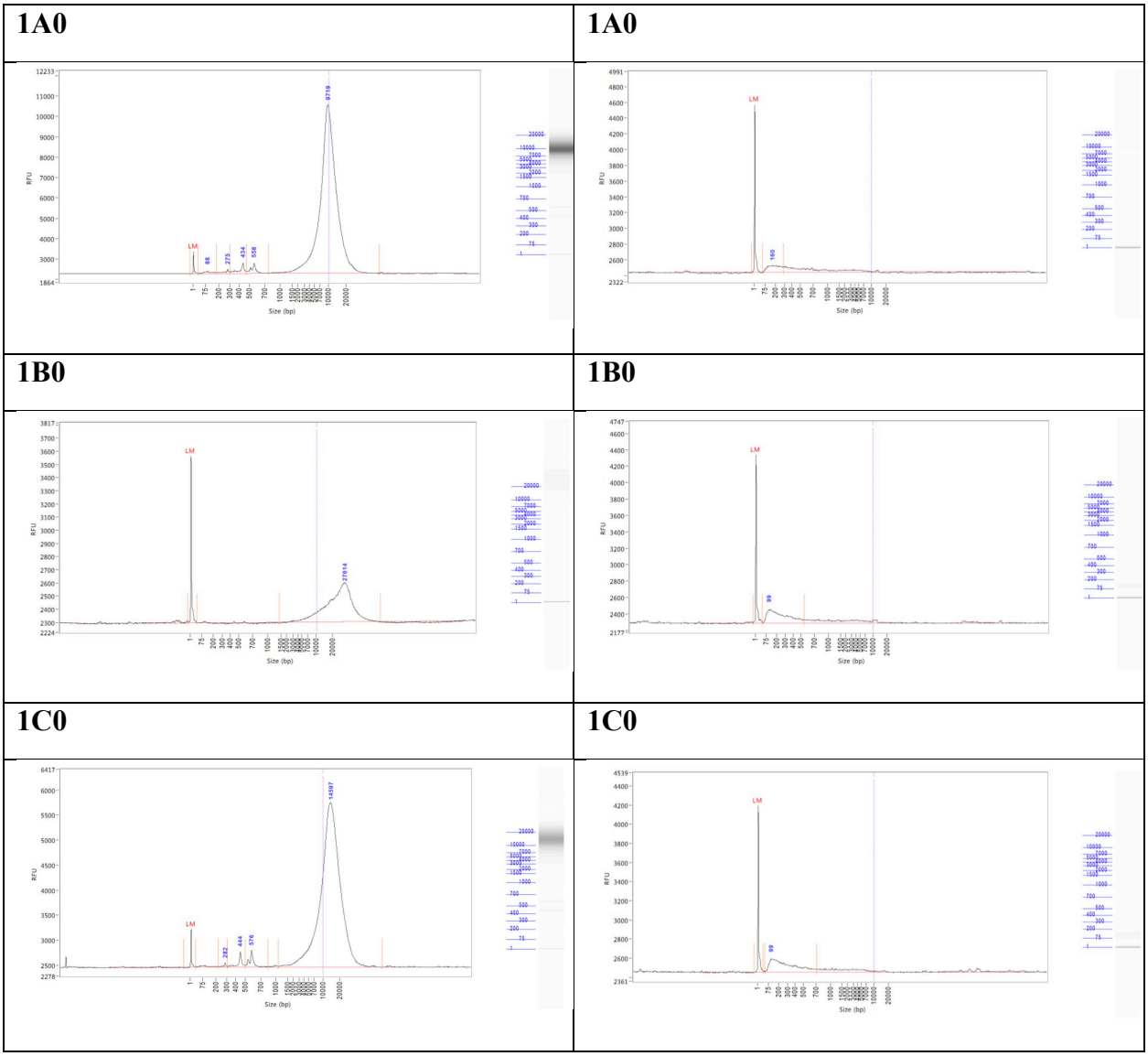

Figure-11: *S. Typhimurium* 13311 Fragment Analyzer Data

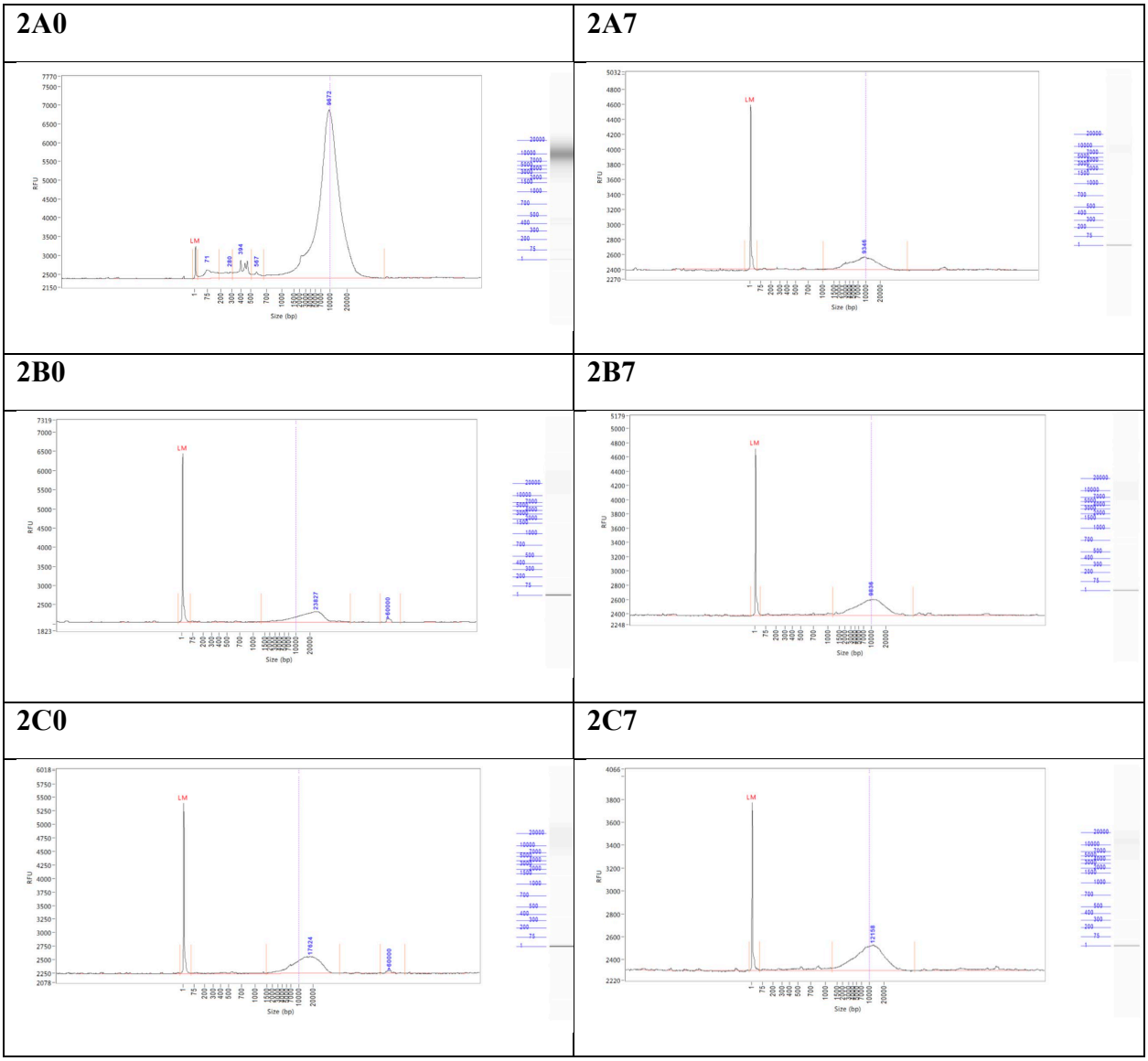

Figure-12: *S. Typhimurium* NVSL87-826254 Fragment Analyzer Data

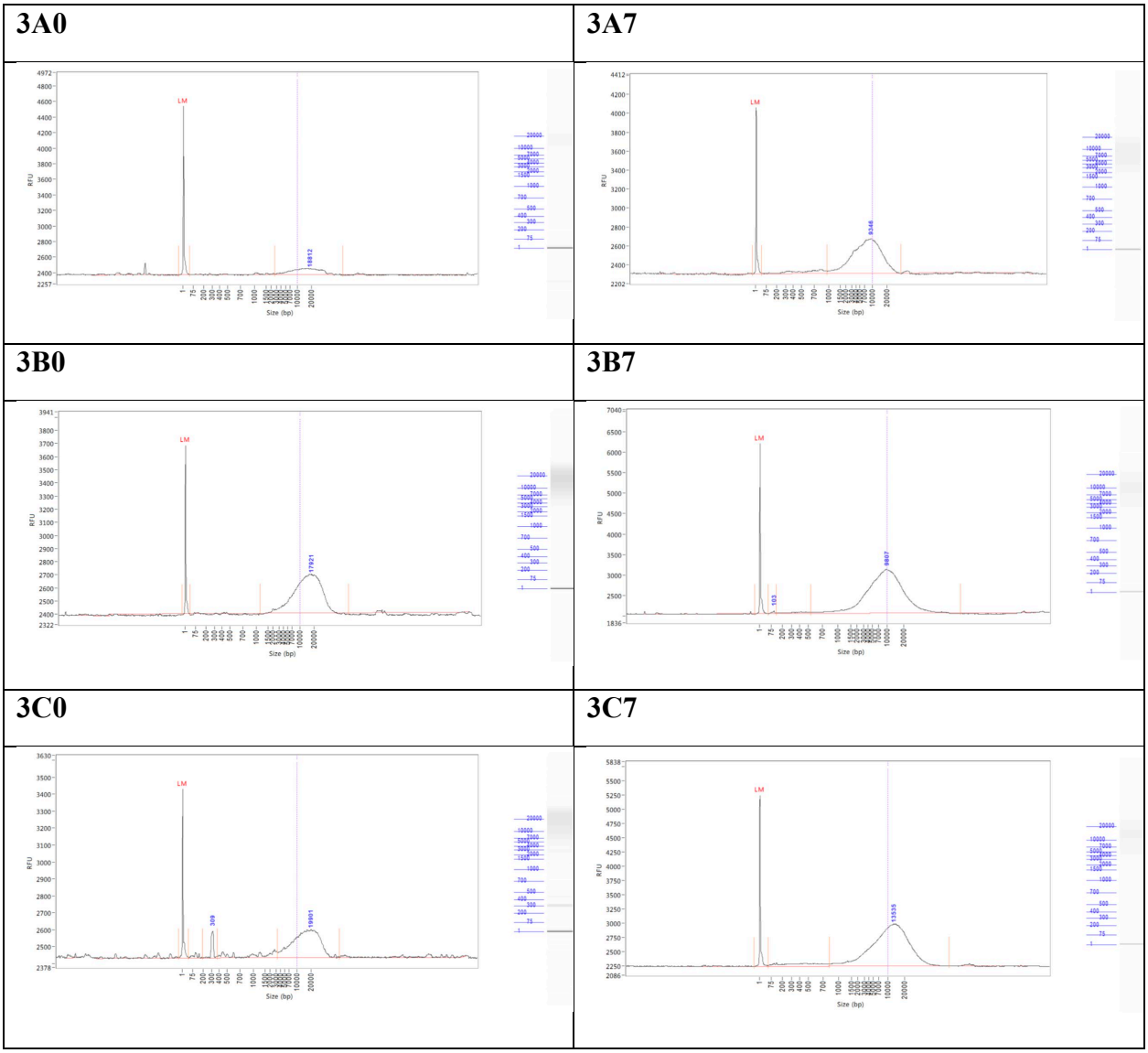

Figure-13: *S. Typhimurium* 12179 Fragment Analyzer Data

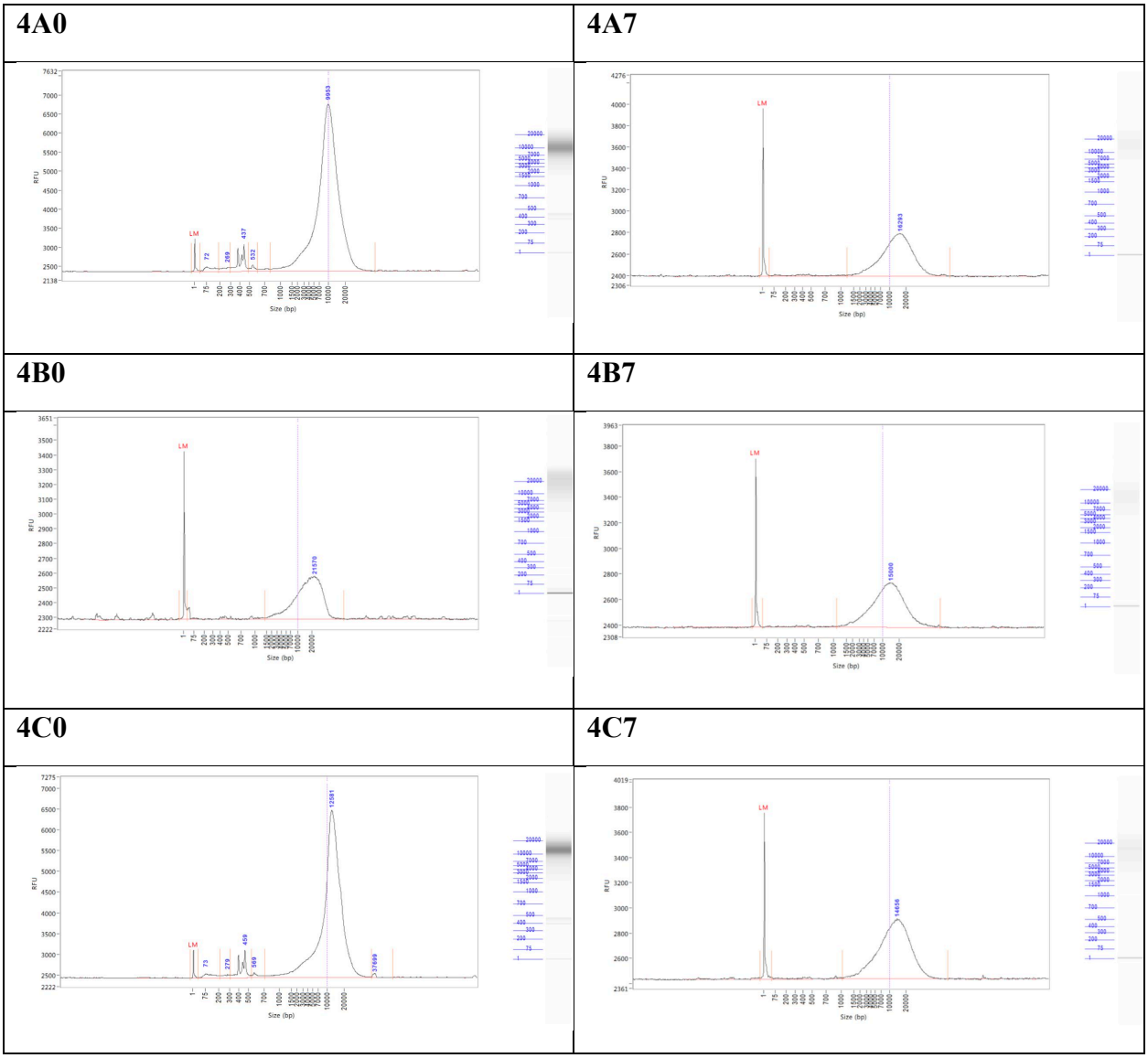

Figure-14: *S. Typhimurium* MET844 Fragment Analyzer Data

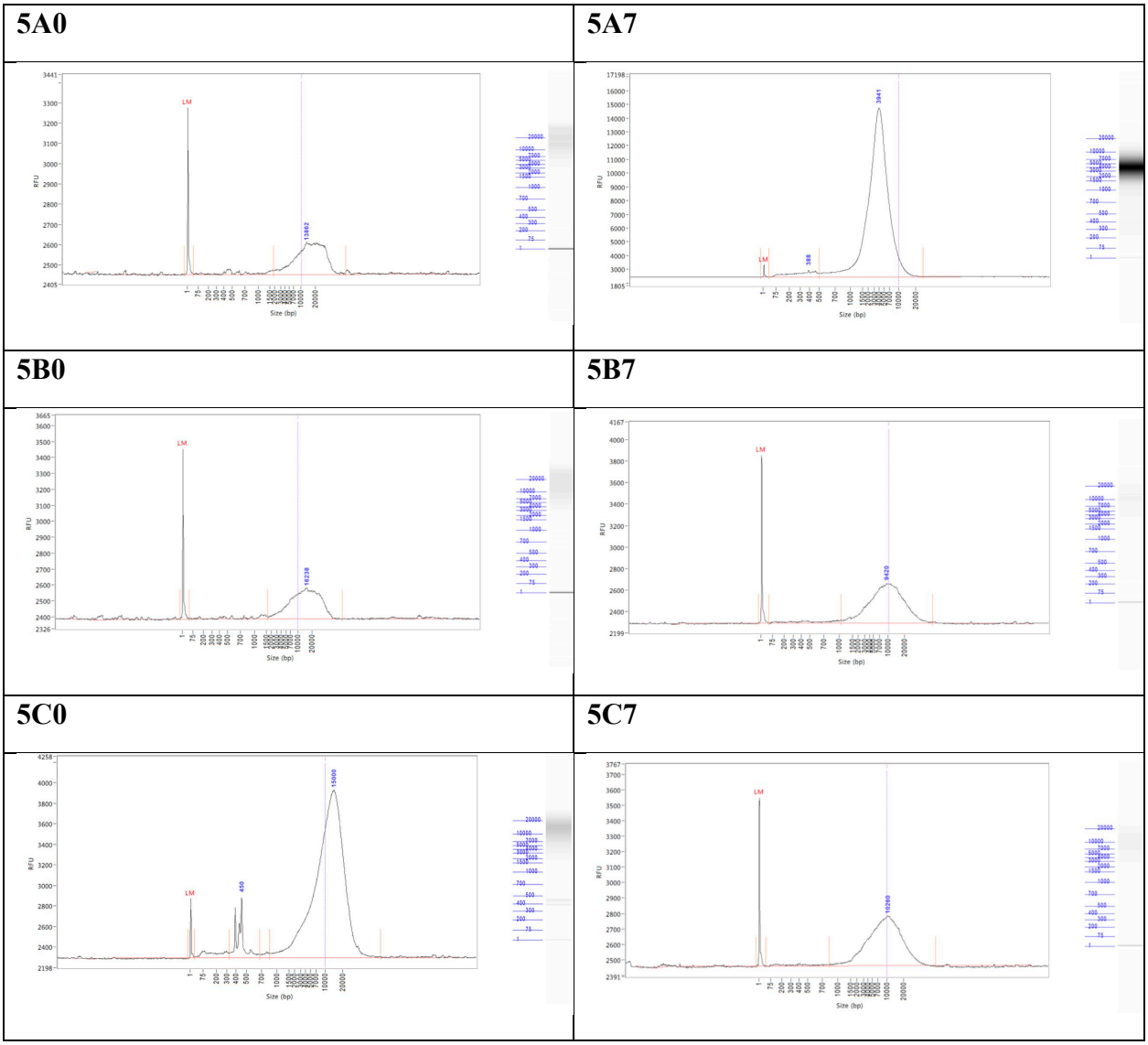

Figure-15: *S. Typhimurium* SS007 Fragment Analyzer Data

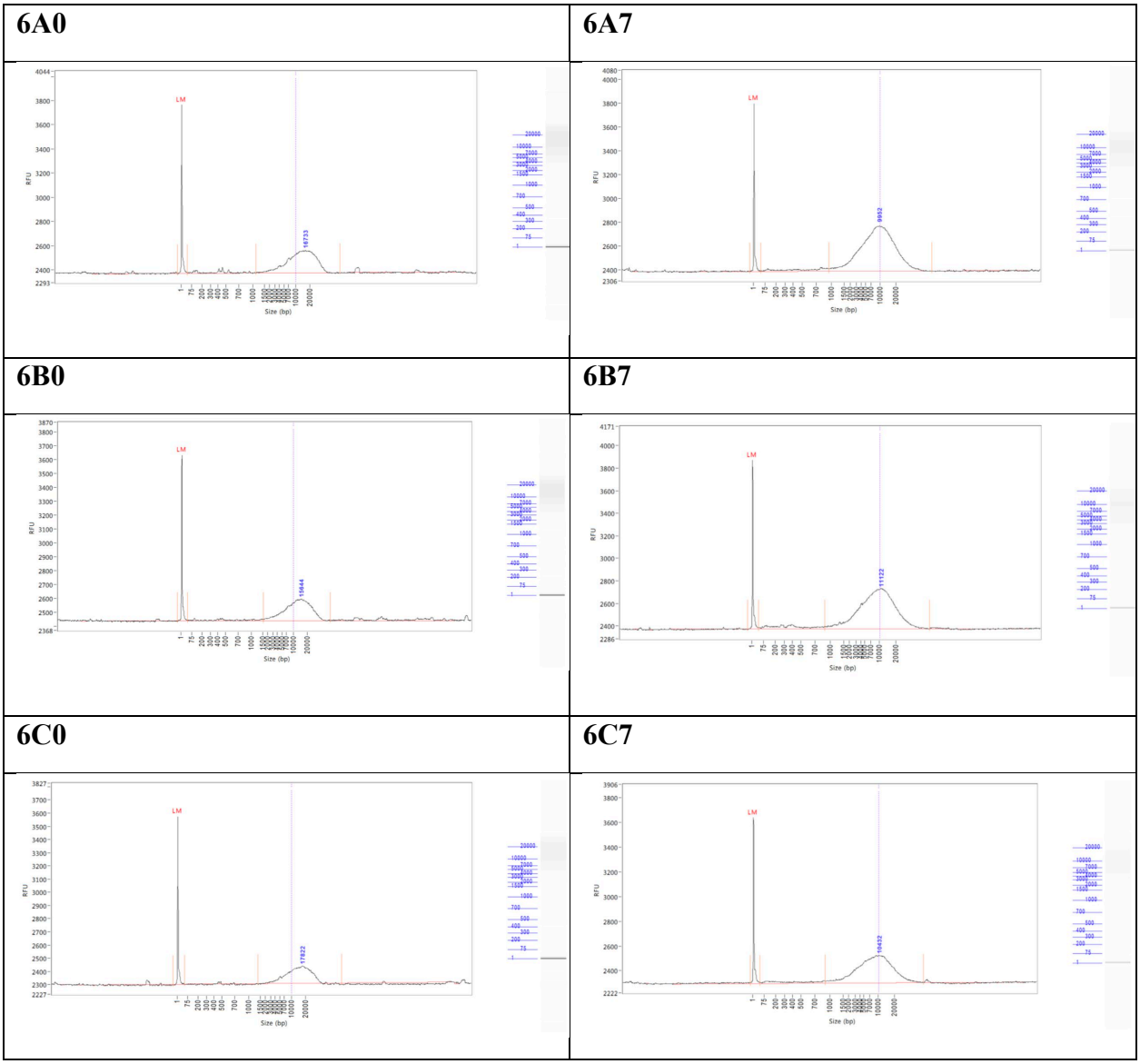

Figure-16: *S. Typhimurium* PJ002 Fragment Analyzer Data

APPENDIX B

Well	ID
1	-
2	1A-0
3	1A-7
4	1B-0
5	1B-7
6	Ladder
7	1C-0
8	1C-7
9	1A-0
10	1B-0
11	1C-0
12	1A-7
13	1B-7
14	1C-7
15	Ladder

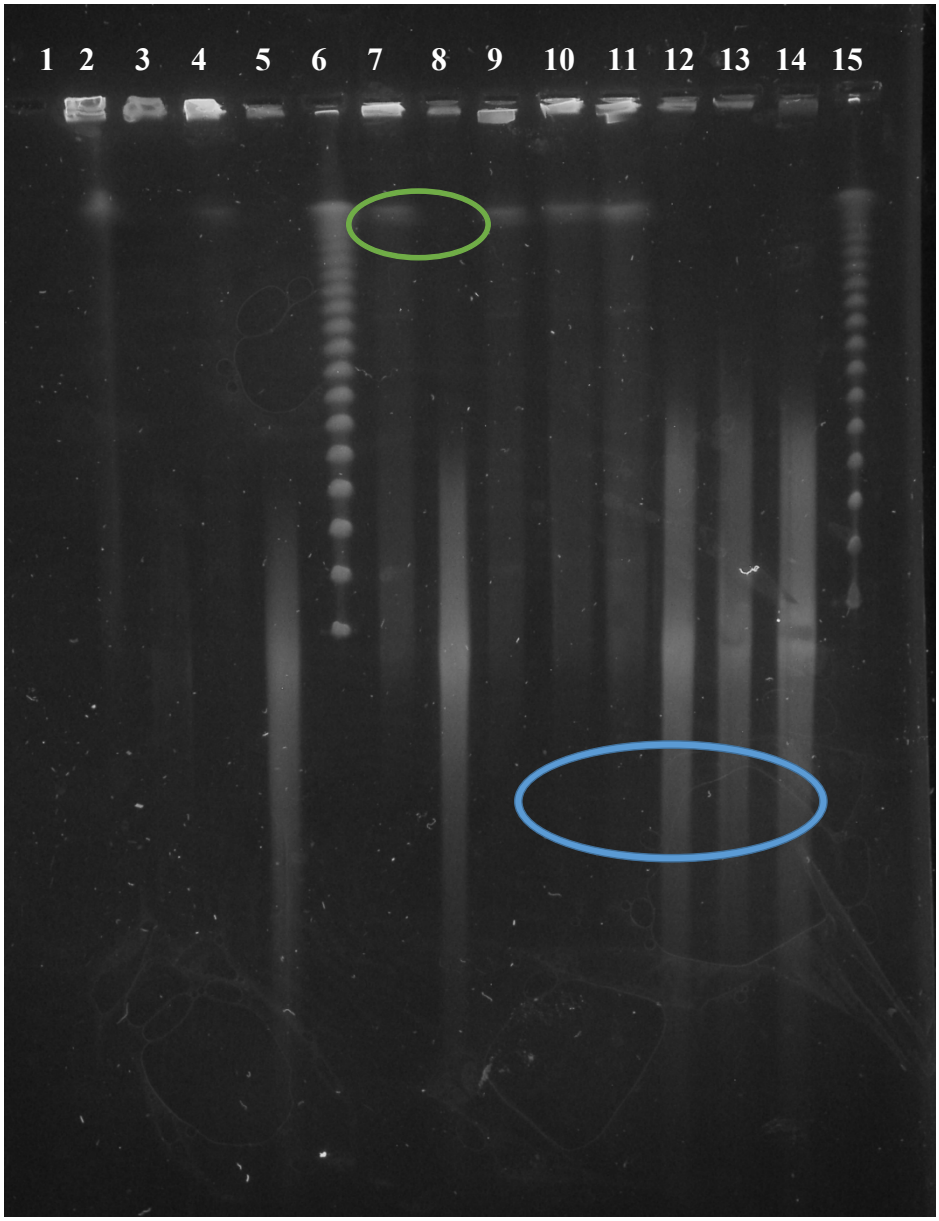

Figure-17: *E. coli* AM076 Pulse Field Gel Electrophoresis. Green circle indicates higher molecular weight fragments; Blue circle indicates lower molecular weight fragments.

Well	ID
1	Ladder
2	2A-0
3	2A-7
4	2B-0
5	2B-7
6	Ladder
7	2C-0
8	2C-7
9	2A-0
10	2B-0
11	2C-0
12	2A-7
13	2B-7
14	2C-7
15	Ladder

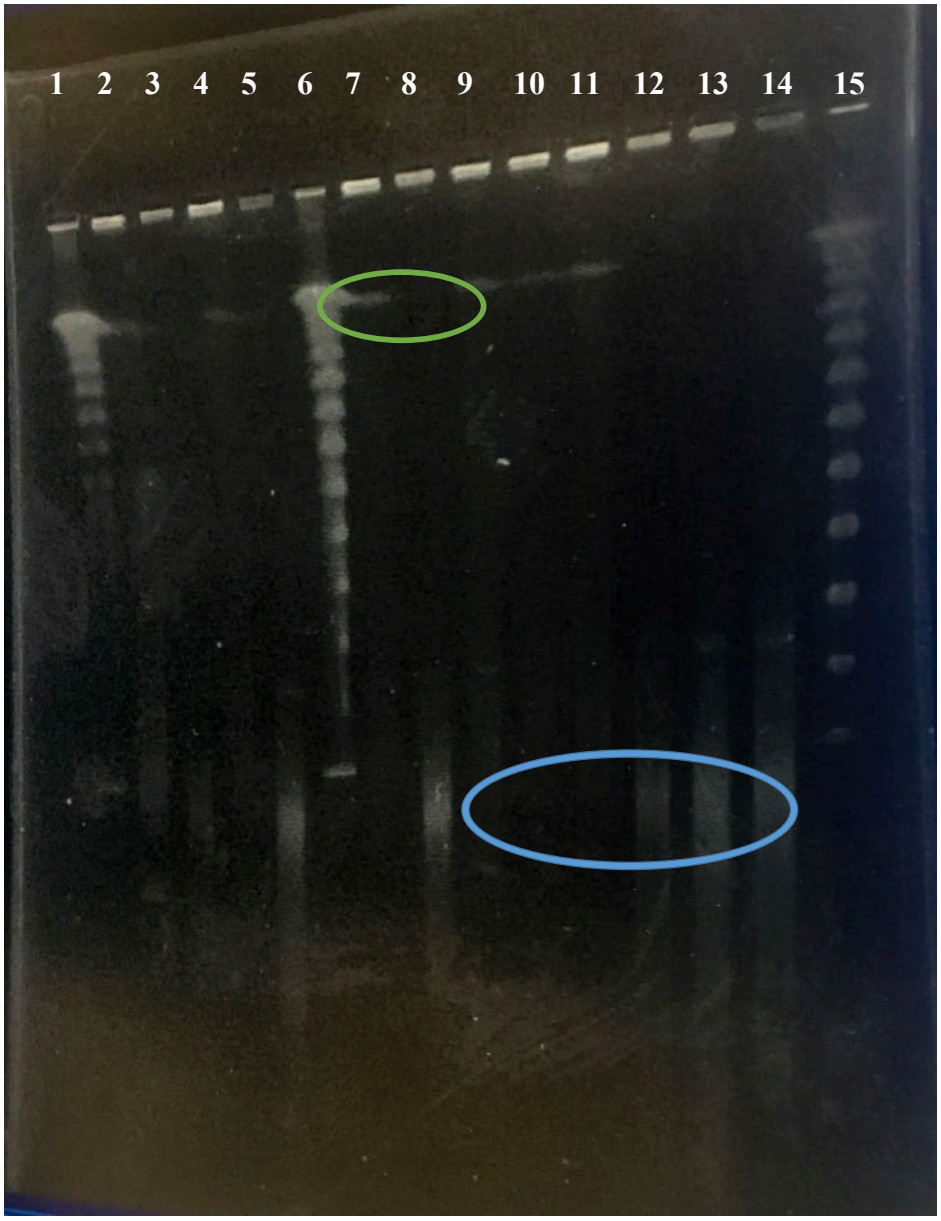

Figure-18: *E. coli* AM1087 Pulse Field Gel Electrophoresis. Green circle indicates higher molecular weight fragments; Blue circle indicates lower molecular weight fragments.

Well	ID
1	-
2	3A-0
3	3A-7
4	3B-0
5	3B-7
6	Ladder
7	3C-0
8	3C-7
9	3A-0
10	3B-0
11	3C-0
12	3A-7
13	3B-7
14	3C-7
15	-

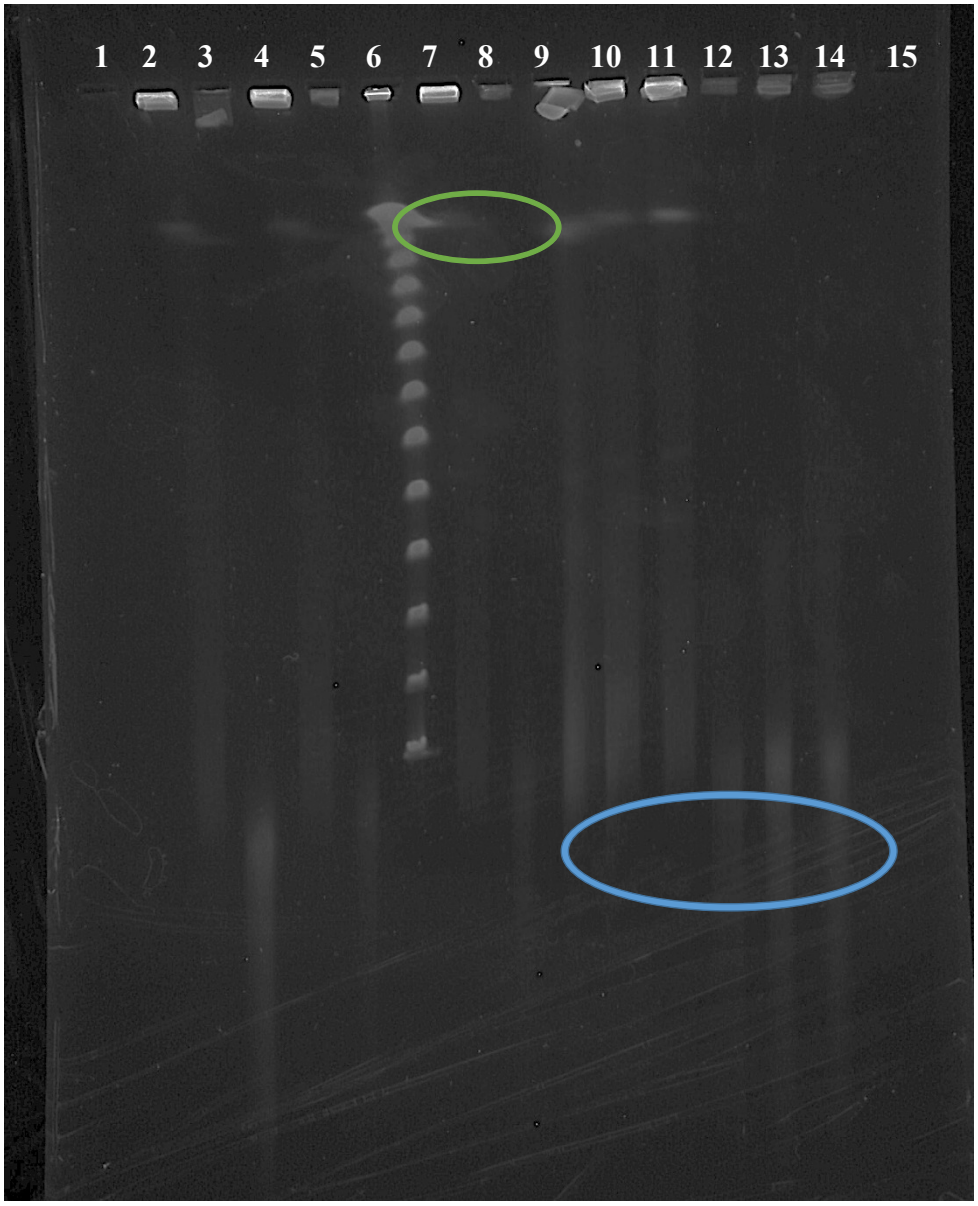

Figure-19: *E. coli* 25922 Pulse Field Gel Electrophoresis. Green circle indicates higher molecular weight fragments; Blue circle indicates lower molecular weight fragments.

Well	ID
1	Ladder
2	4A-0
3	4A-7
4	4B-0
5	4B-7
6	Ladder
7	4C-0
8	4C-7
9	4A-0
10	4B-0
11	4C-0
12	4A-7
13	4B-7
14	4C-7
15	-

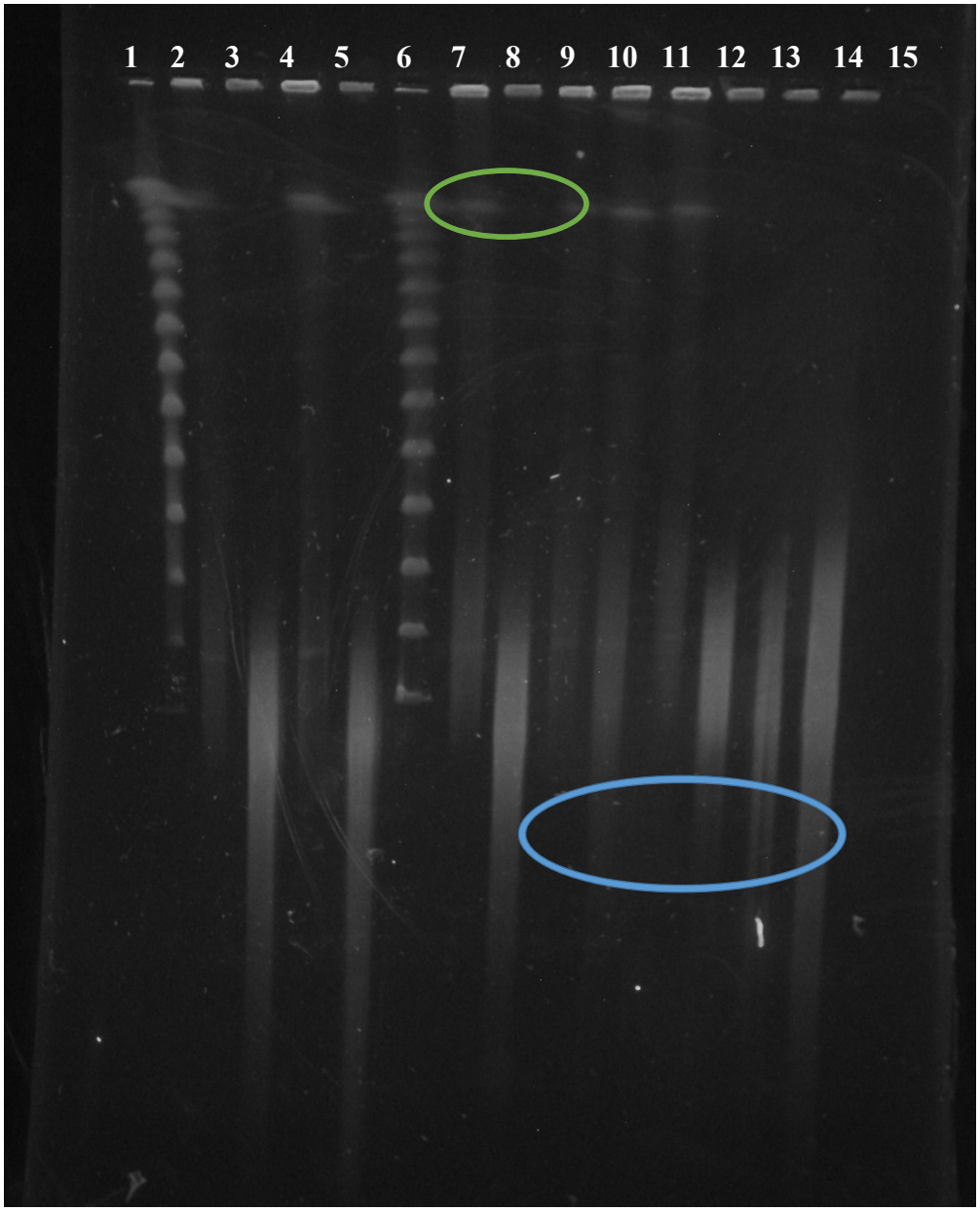

Figure-20: *E. coli* DY330N Pulse Field Gel Electrophoresis. Green circle indicates higher molecular weight fragments; Blue circle indicates lower molecular weight fragments.

***Figure-21: E. coli* 11775 Pulse Field Gel Electrophoresis:**

Well	ID
1	Ladder
2	5A-0
3	5A-7
4	5B-0
5	5B-7
6	Ladder
7	5C-0
8	5C-7
9	5A-0
10	5B-0
11	5C-0
12	5A-7
13	5B-7
14	5C-7
15	-

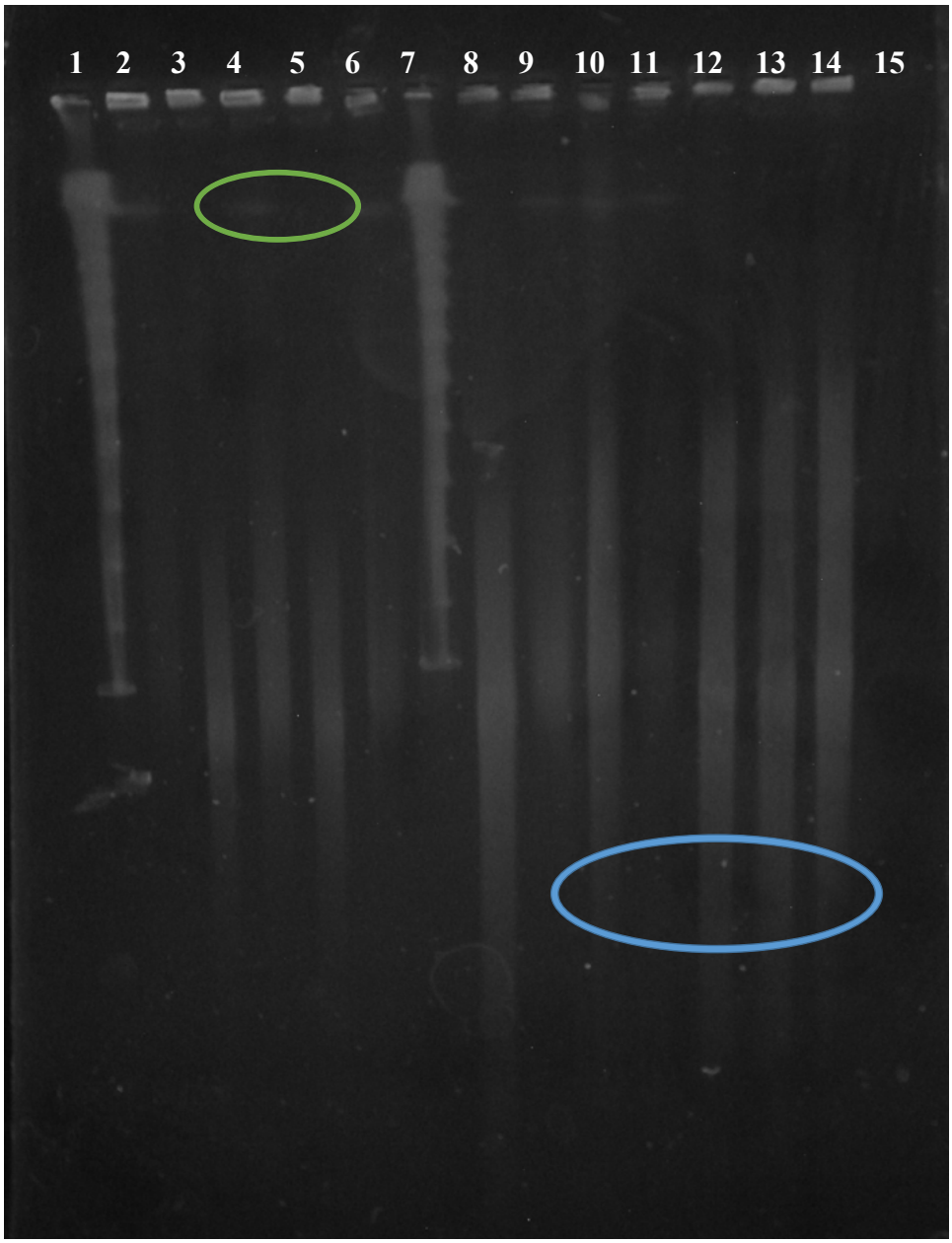

Figure-21: *E. coli* 11775 Pulse Field Gel Electrophoresis. Green circle indicates higher molecular weight fragments; Blue circle indicates lower molecular weight fragments.

Well	ID
1	-
2	6A-0
3	6A-7
4	6B-0
5	6B-7
6	Ladder
7	6C-0
8	6C-7
9	6A-0
10	6B-0
11	6C-0
12	6A-7
13	6B-7
14	6C-7
15	Ladder

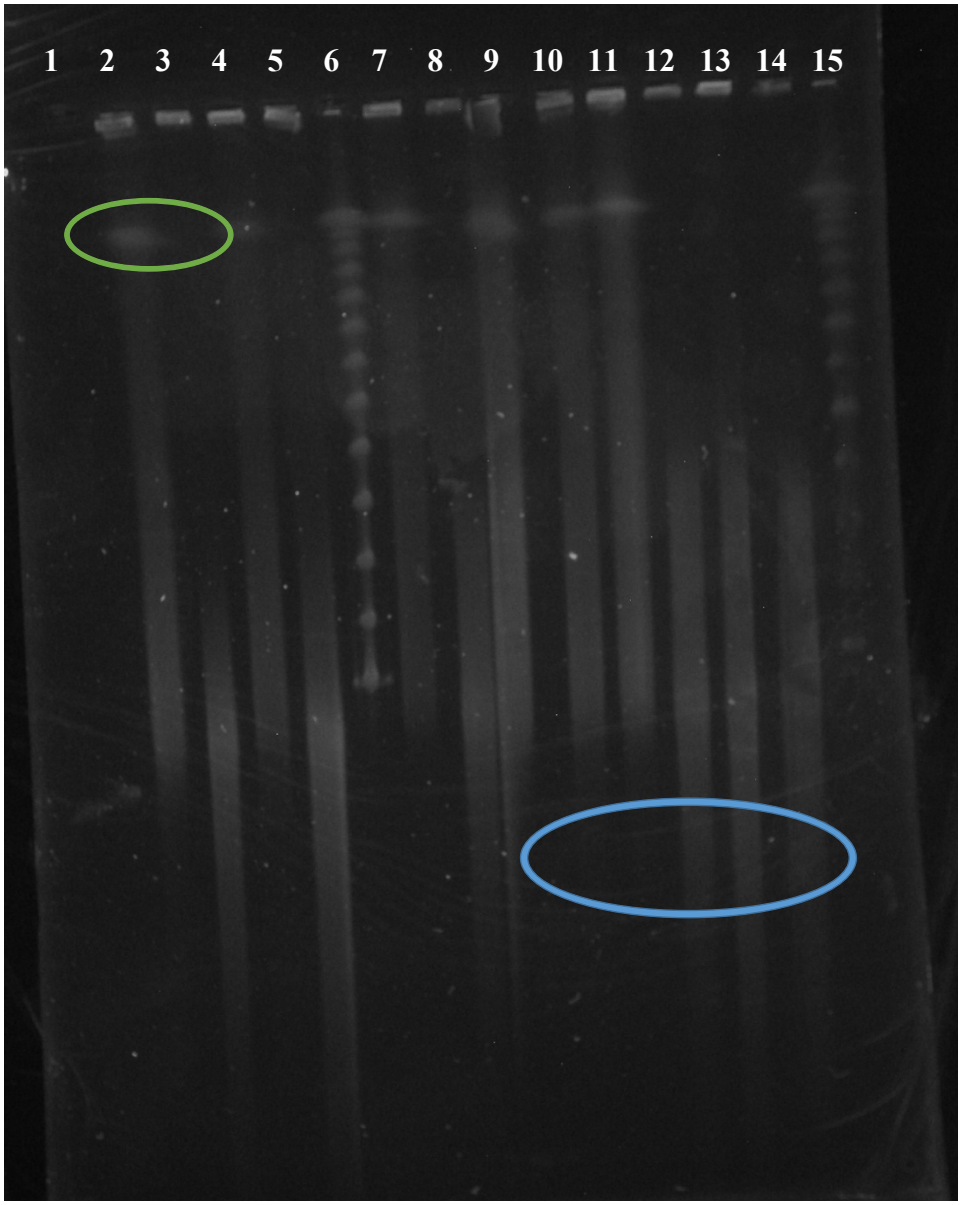

Figure-22*: E. coli* K-12 Pulse Field Gel Electrophoresis. Green circle indicates higher molecular weight fragments; Blue circle indicates lower molecular weight fragments.

Well	ID
1	Ladder
2	1A-0
3	1A-7
4	1B-0
5	1B-7
6	Ladder
7	1C-0
8	1C-7
9	1A-0
10	1B-0
11	1C-0
12	1A-7
13	1B-7
14	1C-7
15	Ladder

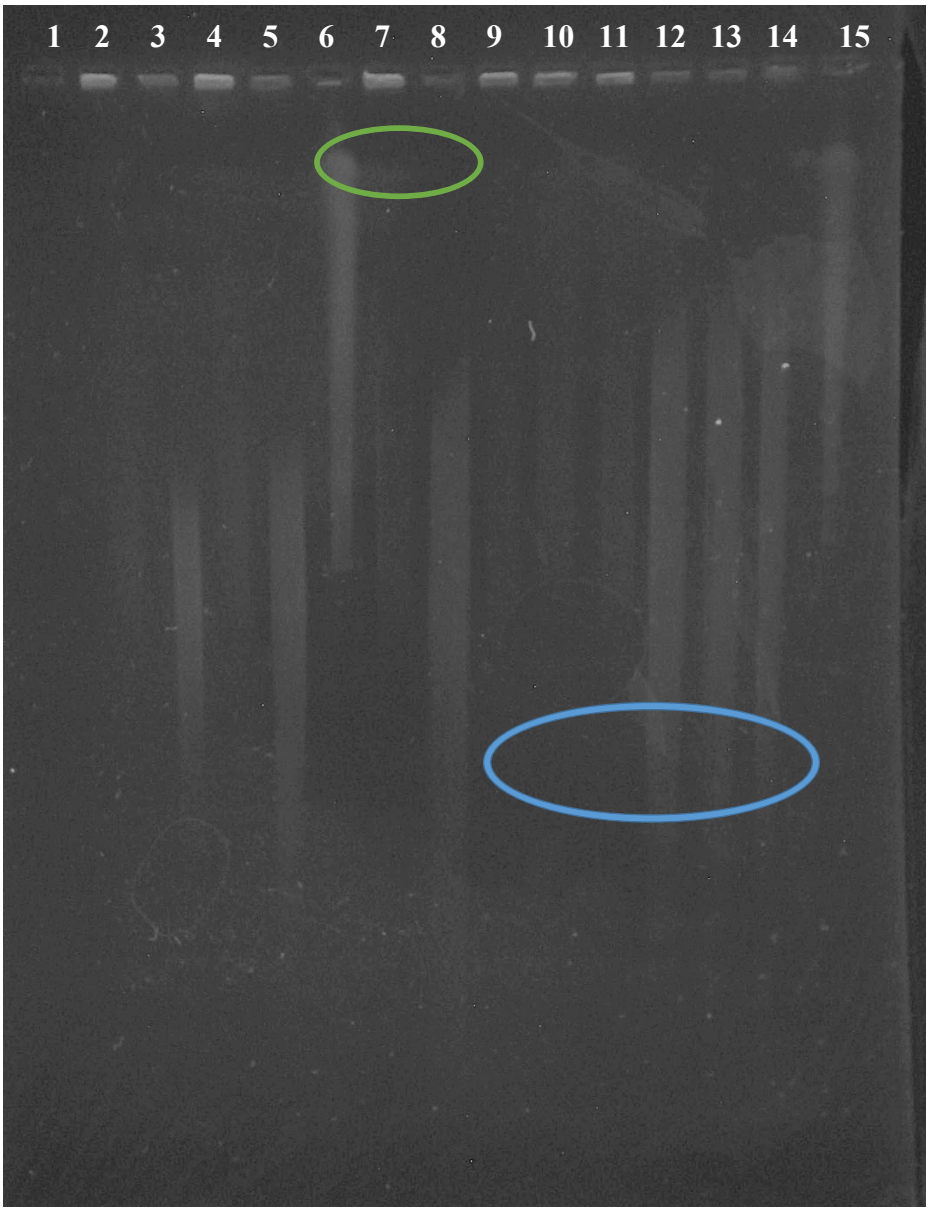

Figure-23*: S. Typhimurium* 113311 Pulse Field Gel Electrophoresis. Green circle indicates higher molecular weight fragments; blue circle indicates lower molecular weight fragments.

Well	ID
1	Ladder
2	2A-0
3	2A-7
4	2B-0
5	2B-7
6	Ladder
7	2C-0
8	2C-7
9	2A-0
10	2B-0
11	2C-0
12	2A-7
13	2B-7
14	2C-7
15	-

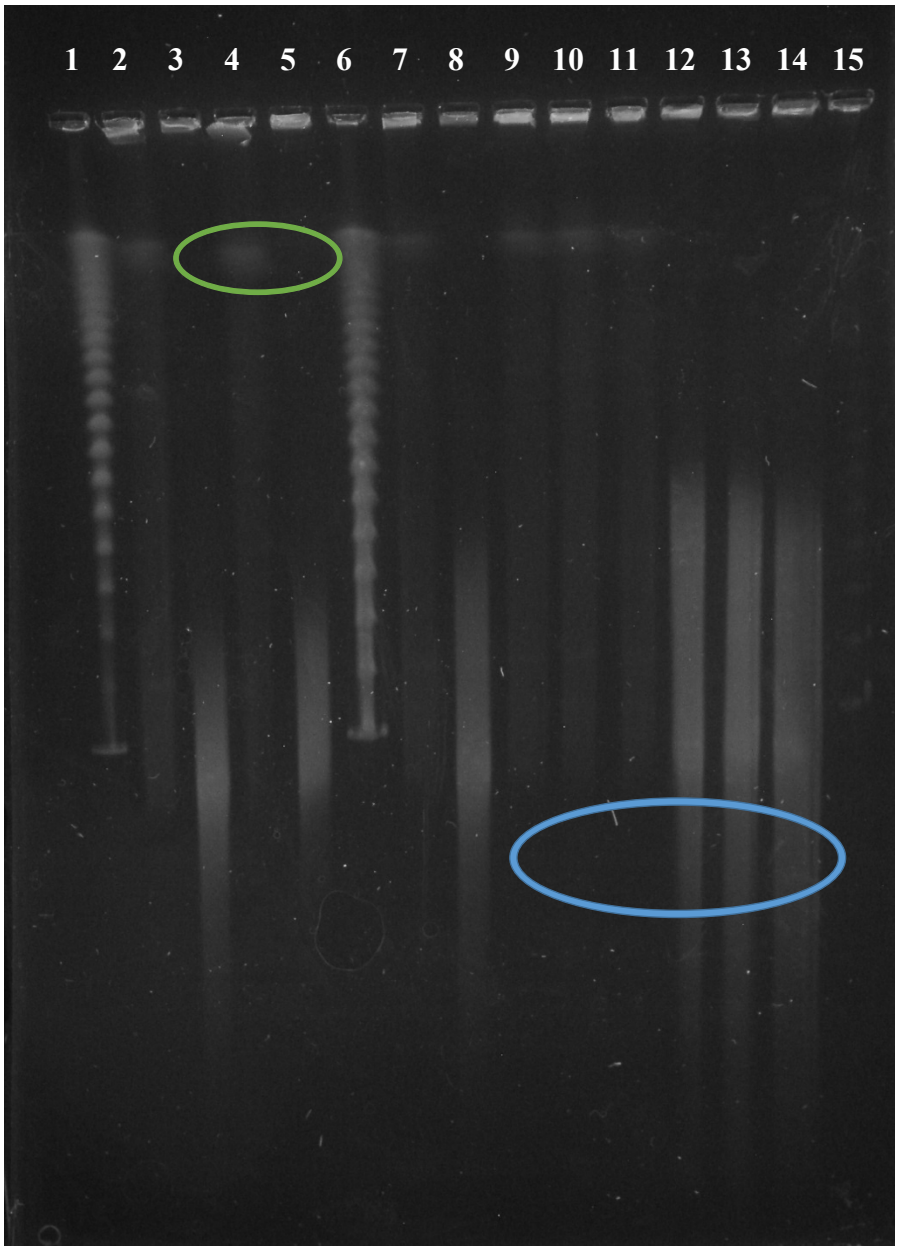

Figure-24*: S. Typhimurium* NVSL87-826254 Pulse Field Gel Electrophoresis. Green circle indicates higher molecular weight fragments; blue circle indicates lower molecular weight fragments.

Well	ID
1	Ladder
2	3A-0
3	3A-7
4	3B-0
5	3B-7
6	Ladder
7	3C-0
8	3C-7
9	3A-0
10	3B-0
11	3C-0
12	3A-7
13	3B-7
14	3C-7
15	-

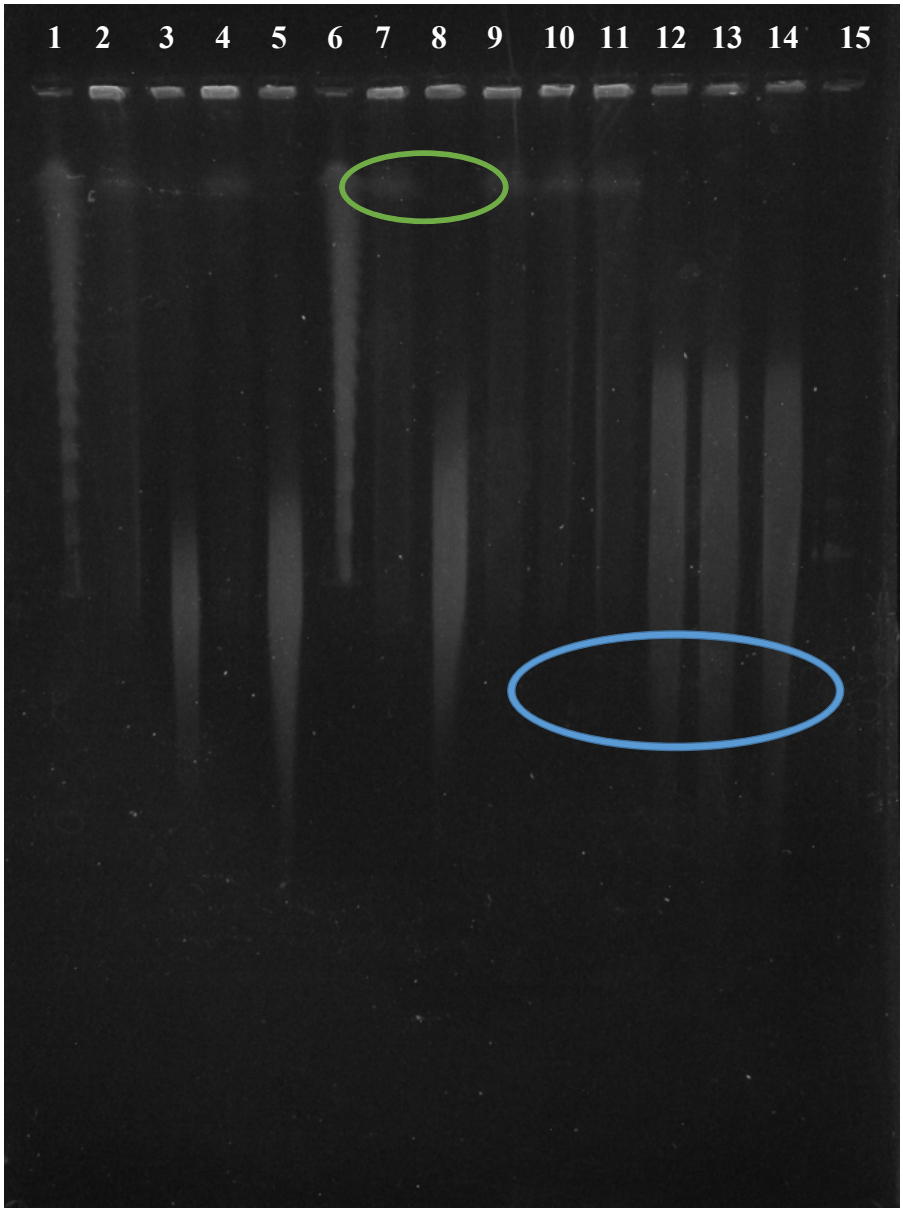

Figure-25*: S. Typhimurium* 12179 Pulse Field Gel Electrophoresis. Green circle indicates higher molecular weight fragments; blue circle indicates lower molecular weight fragments.

Well	ID
1	-
2	4A-0
3	4A-7
4	4B-0
5	4B-7
6	Ladder
7	4C-0
8	4C-7
9	4A-0
10	4B-0
11	4C-0
12	4A-7
13	4B-7
14	4C-7
15	Ladder

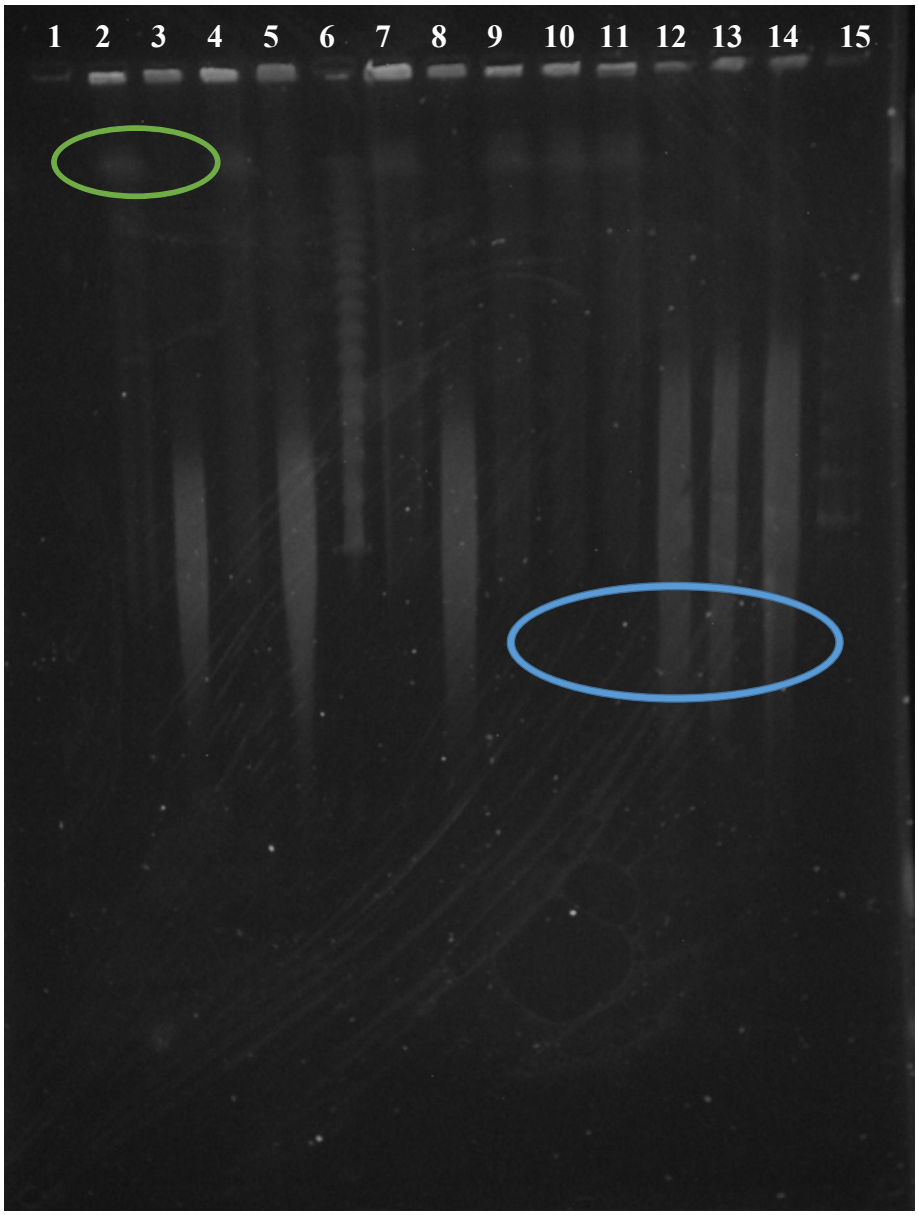

Figure-26*: S. Typhimurium* MET844 Pulse Field Gel Electrophoresis. Green circle indicates higher molecular weight fragments; blue circle indicates lower molecular weight fragments.

Well	ID
1	-
2	5A-0
3	5A-7
4	5B-0
5	5B-7
6	Ladder
7	5C-0
8	5C-7
9	5A-0
10	5B-0
11	5C-0
12	5A-7
13	5B-7
14	5C-7
15	Ladder

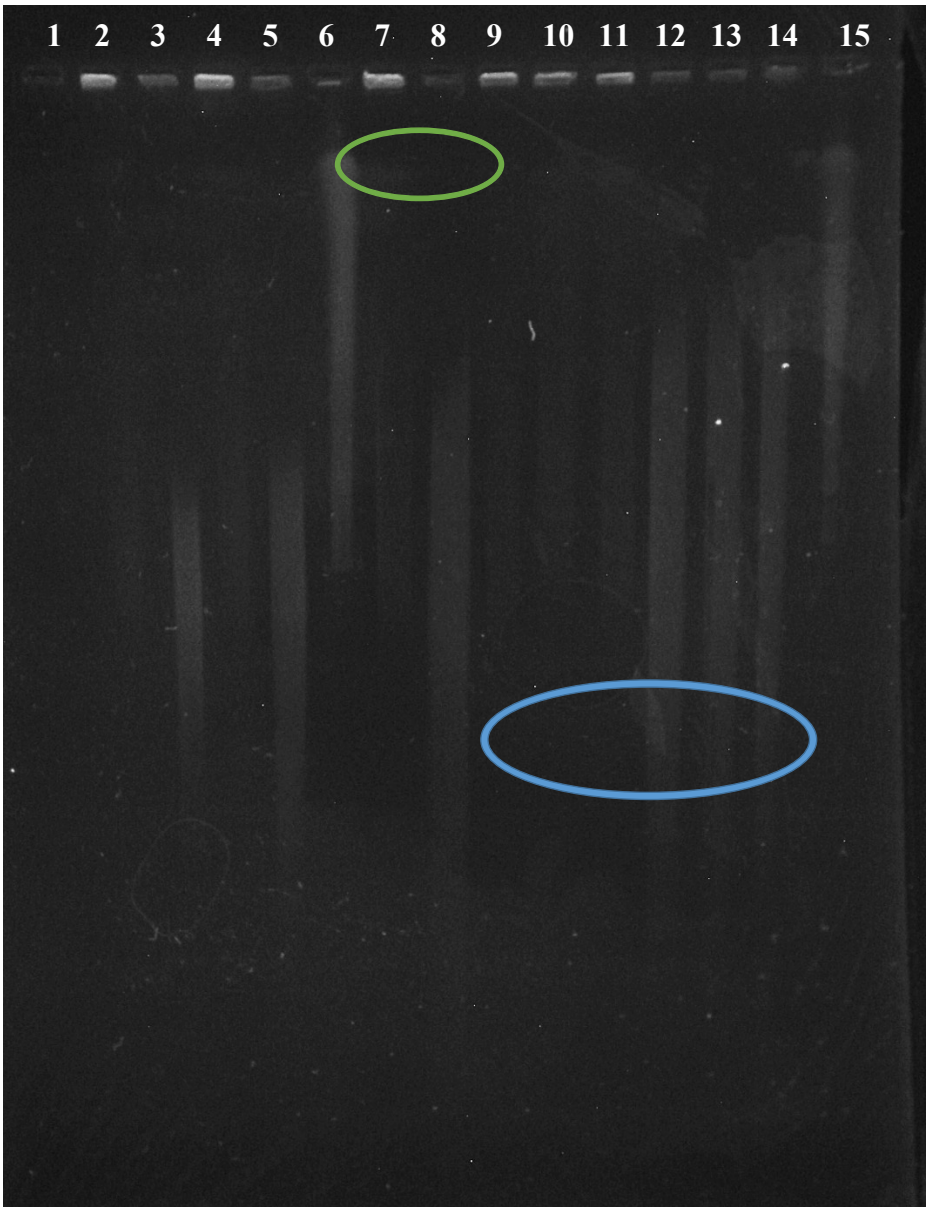

Figure-27*: S. Typhimurium* SS007 Pulse Field Gel Electrophoresis. Green circle indicates higher molecular weight fragments; blue circle indicates lower molecular weight fragments.

Well	ID
1	Ladder
2	6A-0
3	6A-7
4	6B-0
5	6B-7
6	Ladder
7	6C-0
8	6C-7
9	6A-0
10	6B-0
11	6C-0
12	6A-7
13	6B-7
14	6C-7
15	Ladder

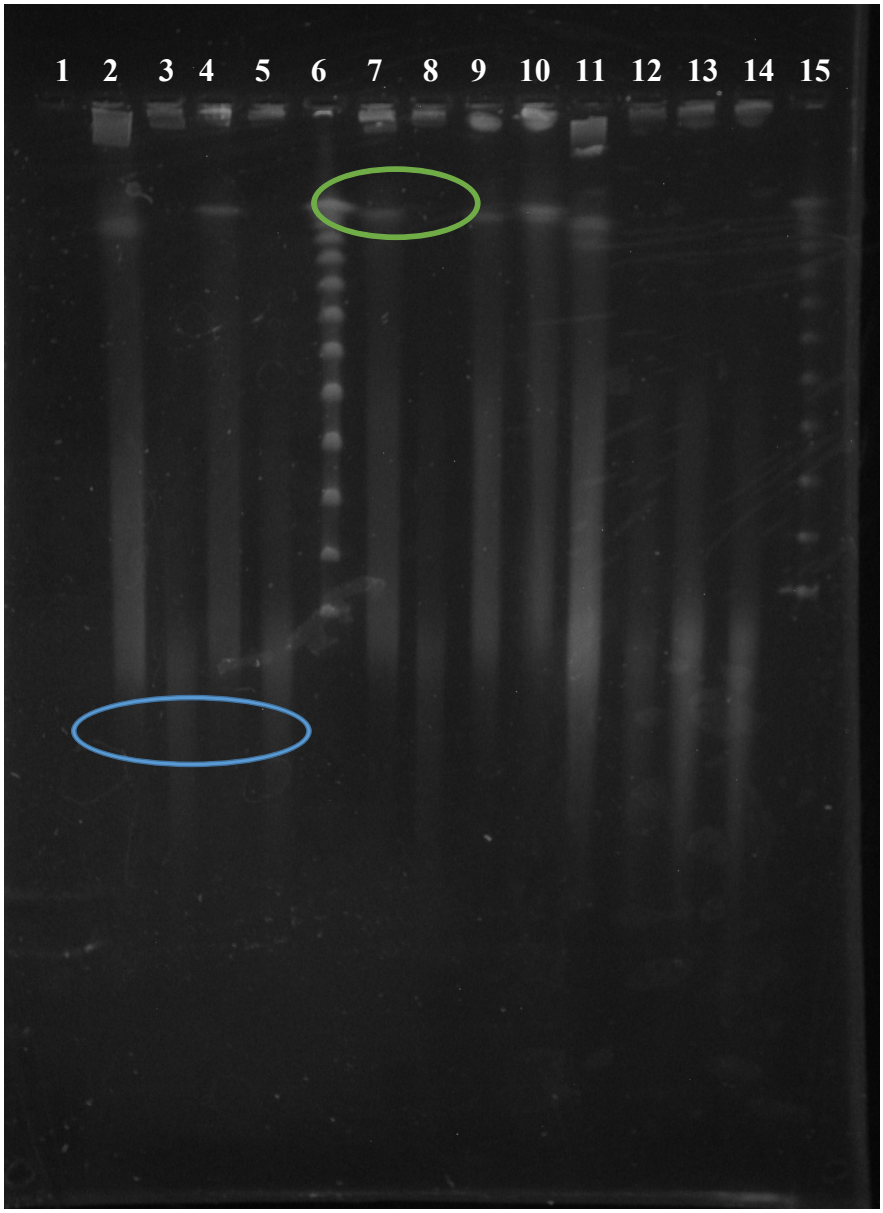

Figure-28: *S. Typhimurium* PJ002 Pulse Field Gel Electrophoresis. Green circle indicates higher molecular weight fragments; Blue circle indicates lower molecular weight fragments.